



**NATURE INSPIRED META-HEURISTICS FOR JPEG
QUANTIZATION TABLE OPTIMIZATION**

PEDRO HENRIQUE GUIMARÃES FERREIRA

**TRABALHO DE CONCLUSÃO DE CURSO EM ENGENHARIA ELÉTRICA
DEPARTAMENTO DE ENGENHARIA ELÉTRICA**

**FACULDADE DE TECNOLOGIA
UNIVERSIDADE DE BRASÍLIA**

**UNIVERSIDADE DE BRASÍLIA
FACULDADE DE TECNOLOGIA
DEPARTAMENTO DE ENGENHARIA ELÉTRICA**

**NATURE-INSPIRED META-HEURISTICS FOR JPEG
QUANTIZATION TABLE OPTIMIZATION**

**APLICAÇÕES DE COMPUTAÇÃO BIO-INSPIRADA PARA O
DESIGN DE TABELAS DE QUANTIZAÇÃO EM COMPRESSÃO JPEG**

PEDRO HENRIQUE GUIMARÃES FERREIRA

ORIENTADOR: DR. EDUARDO PEIXOTO FERNANDES DA SILVA

**TRABALHO DE CONCLUSÃO DE CURSO EM
ENGENHARIA ELÉTRICA**

**PUBLICAÇÃO: PPGEA.TD-001/11
BRASÍLIA/DF: SETEMBRO - 2020**

**UNIVERSIDADE DE BRASÍLIA
FACULDADE DE TECNOLOGIA
DEPARTAMENTO DE ENGENHARIA ELÉTRICA**

**NATURE INSPIRED META-HEURISTICS FOR JPEG
QUANTIZATION TABLE OPTIMIZATION**

PEDRO HENRIQUE GUIMARÃES FERREIRA

**TRABALHO DE CONCLUSÃO DE CURSO SUBMETIDA AO DEPARTAMENTO DE ENGENHARIA
ELÉTRICA DA FACULDADE DE TECNOLOGIA DA UNIVERSIDADE DE BRASÍLIA COMO
PARTE DOS REQUISITOS NECESSÁRIOS PARA A OBTENÇÃO DO GRAU DE BACHAREL.**

APROVADA POR:

**Prof. Dr. Eduardo Peixoto Fernandes da Silva – ENE/Universidade de Brasília
Orientador**

**Prof. Dr. Daniel Guerreiro e Silva – ENE/Universidade de Brasília
Membro Interno**

**Prof. Dr. Diogo Caetano Garcia – FGA/Universidade de Brasília
Membro Externo**

BRASÍLIA, 04 DE SETEMBRO DE 2020.

FICHA CATALOGRÁFICA

FERREIRA, PEDRO HENRIQUE GUIMARÃES;
Nature Inspired Meta-Heuristics for JPEG Quantization Table Optimization [Distrito Federal] 2020.
xii, 52p., 210 x 297 mm (ENE/FT/UnB, Bacharel, Engenharia Elétrica, 2020).
Trabalho de Conclusão de Curso – Universidade de Brasília, Faculdade de Tecnologia.
Departamento de Engenharia Elétrica
1. Compressão de Imagens
3. Algoritmos Genéticos
I. ENE/FT/UnB
2. Otimização Numérica
4. Inteligência Artificial
II. Título (série)

REFERÊNCIA BIBLIOGRÁFICA

FERREIRA, P. H. G. (2020). Nature Inspired Meta-Heuristics for JPEG Quantization Table Optimization . Trabalho de Conclusão de Curso em Engenharia Elétrica, Publicação PPGEA.TD-001/11, Departamento de Engenharia Elétrica, Universidade de Brasília, Brasília, DF, 52p.

CESSÃO DE DIREITOS

AUTOR: Pedro Henrique Guimarães Ferreira

TÍTULO: Nature Inspired Meta-Heuristics for JPEG Quantization Table Optimization .

GRAU: Bacharel ANO: 2020

É concedida à Universidade de Brasília permissão para reproduzir cópias desta trabalho de conclusão de curso e para emprestar ou vender tais cópias somente para propósitos acadêmicos e científicos. O autor reserva outros direitos de publicação e nenhuma parte dessa trabalho de conclusão de curso pode ser reproduzida sem autorização por escrito do autor.

Pedro Henrique Guimarães Ferreira

Departamento de Engenharia Elétrica (ENE) - FT

Universidade de Brasília (UnB)

Campus Darcy Ribeiro

CEP 70919-970 - Brasília - DF - Brasil

— *Who is that on the trenches by
your side?*

— *And does it matter?*

— *More than the war itself.*

Unknown Author

ACKNOWLEDGMENTS

Most of all, I would like to dedicate it to my extraordinary family. To my mother, Célia, for being the kindest and caring person I ever knew. To my brother, Eduardo, for being there with me during all these years and to my father, Francisco, for being my biggest supporter. And also to my Canadian Family. To my Godparents, Maida and Eduardo, for showing me that family is not always blood, and to my Godbrother, Lucas, for being the silver lining of most of my clouds.

To my cousins Beatriz, Marcelo, Rafaela, Ricardo, and Sabrina. Especially to Marcelo and Ricardo, for helping me whenever I needed, and to Rafaela, for sharing with me the burdens of college life.

To my lifetime friends Caio, Gabriel, Gustavo, Henrique, Iwar, João Eduardo, João Pedro Lyra, Lucas Carvalho, Lucas Lacerda, Pedro Neff, Pedro Pinheiro and Victor for always encouraging and lifting me up. Twelve years ago, I walked into an empty classroom alone, and, ever since, you have been making my days better and better.

To the friends that UnB brought to my life: André Seiki, Arthur, Allan, Edson, Felipe, Gabriel Lins, Gabriel Soutinho, Hiandra, Isaque Borges, João Foltran, Luis Filomeno, Marcelo, Osmar, Pedro Caio, Pedro Cardoso, Rafael, Rodrigo Borba, Rodrigo Fischer, Sérgio Bittencourt, Tiago Rodrigues, Thiago Dantas, Victor Passamani and Vinicius Jadiscke. You have all my love and gratitude for our outbacks, barbecues, soccer matches, discussions, researches, and study groups. No one could have done it better than you and I am very proud to call you my fellow engineers. A special thanks to my dear friends André Seiki, Arthur, Gabriel Lins, João Foltran, Osmar, Marcelo, Pedro Caio and Thiago Dantas for converting our professional collaborations in astonishing personal enhancement opportunities.

To André Costa, Arthur Sandoval, Clarissa, Gabriel Bertone, Guilherme Shimbuko, Gustavo Leão, Tainan, and Thiago Magalhães for mentoring me, showing me the right paths at UnB and helping me to broaden my own horizons.

To Luiza Farnese, Matheus Noschang, Rubens Braz and Túlio Trefzger for not only for sharing and supporting my biggest dreams as an Electrical Engineering student but also for having the biggest hearts in our course.

In professional terms, I want to dedicate this work to all the staff and faculty of both Departamento de Engenharia Elétrica of Universidade de Brasília and Faculty of Computer Science of Dalhousie University.

To this thesis' supervisor, Dr. Eduardo Peixoto, for being a very committed, hard-working, available, wise, supporting, and understanding supervisor. I feel that your supervision not only enlightened this work, but also made all the hours that I spent on it far more rewarding. Our amazing university is defined by extraordinary people like you.

To my Dalhousie University supervisor, Dr. Nur Zincir-Heywood, and co-supervisor, M.Sc. Duc Le, for the kindness, enthusiasm, availability, support, and teachings over in my stint at Dal. It was by far my best experience at university. I am counting the hours to rejoin the NMIS.

To my former research supervisors, Dr. Felipe Vigolvino and Dr. Cláudia Abbas, for the patience, commitment, teachings, support, and, mainly, to make me enhance. Your experience and guidance had a lot of impact on me.

To Dr. Ricardo Zelenovsky, not only for choosing me as a Teacher Assistant five times in a row but also for being my biggest inspiration and counselor at Universidade de Brasília, as the most gifted lecturer and the smartest and most altruistic person I met in our university. I can only hope to be half the Engineer you are.

To Dr. Alex da Rosa, Dr. Flávio Elias, Dr. Kléber Melo, Dr. João Luiz Carvalho, Dr. João Paulo Leite, Dr. José Edil and Dr. Paulo Portela for the amazing courses that pushed me to the edge, forcing me to think outside the box, and the even better conversations and discussions that made me grow a lot.

To Ms. Vera Simões for being very caring and for helping me countless times.

To Mitacs, for the trust and funds, and to my fellow Mitacs Alumni at Universidade de Brasília, Jean and Isabelle, for our unlikely, but super delightful friendship, and to the Mitacs GRI Alumni at Dalhousie University, especially my Brazilian-Canadian friends Lucas and Vinícius, for making my days better back in Halifax in uneven ways - I still miss cheering for Brazil National Team in the Women's World Cup or going out to fancy dinners in the middle of the week.

To my associate partners at ORA AI, Markus Rosa, and Mitikazu Lisboa, for the trust and collaboration.

RESUMO

Título: Aplicações de Computação Bio-Inspirada para o Design de Tabelas de Quantização em Compressão JPEG

Autor: Pedro Henrique Guimarães Ferreira

Orientador: Dr. Eduardo Peixoto Fernandes da Silva

Programa de Graduação em Engenharia Elétrica

Brasília, 04 de setembro de 2020

Imagens digitais estão cada vez mais presentes em nossa vida cotidiana, respondendo, entre imagens e vídeos, por mais de 75% do tráfego da Internet. Por isso, encontrar formas apropriadas para que as imagens digitais sejam representadas se torna uma necessidade, de forma em que uma adoção massiva de representações compactas de imagens implicaria não somente em uma redução no tempo de carregamento de boa parte das páginas da Internet, mas também do consumo de largura de banda.

Múltiplas técnicas foram propostas para gerar representações de imagens digitais eficientes em memória, dentre as quais destaca-se o JPEG que, embora tenha sido proposto há mais de 25 anos, permanece soberano como o mais adotado padrão de compressão de imagens.

O padrão JPEG estabelece que uma representação eficiente da imagem é obtida a partir de um procedimento de quatro etapas: inicialmente, a imagem a ser comprimida é dividida em blocos de tamanho 8×8 sendo, em seguida, aplicada uma transformação reversível, como, por exemplo, a transformada discreta de coseno. Na sequência, os blocos transformados são quantizados de acordo com os níveis de quantização estabelecidos em uma tabela de quantização. Por fim, os valores quantizados são reorganizados em um procedimento denominado *zigzag scan* e, em seguida, submetidos à um codificador de entropia.

É importante ressaltar que, em geral, a quantização é a etapa crítica do processo de compressão, uma vez que se trata da única etapa irreversível, sendo tanto a única etapa onde se a distorção, quanto a etapa preponderante na redução da taxa da imagem, de forma em que a taxa obtida está fortemente relacionada com a magnitude dos coeficientes de quantização utilizados.

Nesse trabalho, propõe-se a aplicação de dois algoritmos de computação bio-inspirada, nominalmente *Particle Swarm Optimization* e *Dual Simulated Annealing*, para a geração de tabelas de quantização personalizadas, específicas para cada imagem, buscando obter uma melhor relação entre a taxa de compressão obtida e a qualidade da imagem reconstruída. Para isso, uma nova métrica, denominada Ganho de Taxa Esperado para uma mesma qualidade (FQ-ERG), também é proposta.

Os resultados experimentais verificam a validade das técnicas propostas, permitindo que uma redução no tamanho das imagens comprimidas de até 8% sem perda de qualidade seja obtida em uma quantidade moderada de tempo.

Palavras-chave: Compressão de Imagem, Computação Bio-Inspirada, Otimização Numérica, Quantização

ABSTRACT

Title: Nature-Inspired Meta-Heuristics for JPEG Quantization Table Optimization

Author: Pedro Henrique Guimarães Ferreira

Supervisor: Dr. Eduardo Peixoto Fernandes da Silva

Graduate Program in Electrical Engineering

Brasília, September 4th, 2020

Digital Images are present everywhere in our daily life. Combined, still and motion images represent more than 75% of the global web traffic. Therefore, the way how digital images are represented has a considerable impact in terms of resource consumption.

Memory efficient image representations have been an important research topic for years since the widespread adoption of compact image representations can both speed up page loading and shrink the bandwidth consumption. For this purpose, multiple image compression standards were proposed, with the JPEG standard standing up as the most widely adopted compression technique for still images.

In JPEG, image compression is achieved by splitting an image into tiles, applying a transform on each block, then quantizing the transformed blocks and reordering and entropy coding its coefficients. On JPEG, both the amount of compression obtained and the quality loss originated from this process are closely related to the choice of the quantization levels for the quantization stage, which are often represented as tables called quantization table.

This work proposes the adoption of two nature-inspired meta-heuristics, Particle Swarm Optimization and Dual Simulated Annealing, to optimize quantization tables in JPEG compression, aiming to find quantization tables that provide enhanced rate-distortion compromises. For this purpose, a new rate-distortion metric, Fixed Quality Expected Rate Gain (FQ-ERG), is specifically designed and employed alongside the classical Lagrangian cost function. Since the JPEG standard has support to custom quantization tables, the product of this process is an optimized, but still JPEG compliant image.

Our results reveal that the proposed approach can obtain state-of-the-art results, with both Particle Swarm Optimization and Dual Simulated Annealing managing to outperform the baseline JPEG by reducing the compressed file size at an average of 8% for same quality images, while the newly proposed metric FQ-ERG was verified to be a suitable metric for quantization table optimization, contributing to a 4% performance improvement for DSA in comparison with the classical Lagrangian cost function, while presenting a similar performance for PSO.

Keywords: Image Compression, Nature Inspired Heuristics, Numerical Optimization, JPEG Quantization Tables

SUMMARY

1 INTRODUCTION AND RELATED WORK	1
1.1 INTRODUCTION	1
1.2 RELATED WORK	2
2 THEORETICAL FRAMEWORK.....	4
2.1 DIGITAL IMAGE REPRESENTATION	4
2.1.1 COLOR SPACES	4
2.1.1.1 RGB COLOR SPACES.....	5
2.1.1.2 YC_bC_r COLOR SPACE	6
2.1.1.3 COLOR SPACE CONVERSION	7
2.2 IMAGE COMPRESSION	7
2.2.1 THE JPEG STILL PICTURE COMPRESSION STANDARD	8
2.2.2 JPEG QUANTIZATION TABLE	10
2.2.3 COMPRESSION RATE	11
2.2.4 IMAGE RATE	12
2.2.5 MEAN-SQUARED ERROR.....	12
2.2.5.1 PEAK SIGNAL-TO-NOISE RATE	13
2.2.6 LAGRANGIAN RATE-DISTORTION COST FUNCTION	13
2.2.7 BJØNTEGAARD DELTA METRIC	14
2.3 NUMERICAL OPTIMIZATION	15
2.3.1 PARTICLE SWARM OPTIMIZATION (PSO).....	16
2.3.2 DUAL SIMULATED ANNEALING (SA)	17
3 METHODOLOGY	18
3.1 QUANTIZATION TABLE OPTIMIZATION.....	18
3.2 QUANTIZATION TABLE REPRESENTATION	20
3.3 INITIAL GUESS	21
3.4 FITNESS FUNCTIONS.....	22
3.4.1 THE FIXED QUALITY EXPECTED RATE GAIN (FQ-ERG)	23
3.5 IMPLEMENTATIONS	25
4 RESULTS	27
4.1 SETTINGS.....	27
4.2 NUMERICAL EVALUATION	28
4.3 TIME PERFORMANCE	33
4.4 VISUAL ASSESSMENT	35

SUMMARY	ix
5 CONCLUSION AND FUTURE WORK.....	40
REFERENCES	41
A RATE-DISTORTION CURVES ON KODAK DATASET	48

LIST OF FIGURES

2.1	An Example of a Digital Image [1]	4
2.2	A RGB image can be decomposed on three channels or bands: a red, a green and a blue.....	5
2.3	Decomposition of a colored Image (upper left) into its YC_bC_r channels, the luminance (upper right) and the C_b and C_r chrominance (lower left and right) components	6
2.4	A Block Diagram representation of the JPEG Encoding Process.....	8
2.5	A Block Diagram representation of the JPEG Decoding Process	9
2.6	The Zig-Zag Scan Order	10
2.7	Two rate-distortion curves represented in the same figure: The Bjøntegaard Delta is numerically equivalent to the filled area	14
3.1	Fluxogram of the nature inspired metaheuristic behaviour on optimizing JPEG quantization tables	19
3.2	Quantization Table Pre-Processing Process	20
3.3	Graphical Representation of the Expect Rate Gain for a given operation point: The ERG corresponds to the ratio between the actual point rate, R, and the projected rate to baseline JPEG produce a same quality image, E(D)...	24
4.1	The Kodak Image Dataset	27
4.2	Rate-Distortion Curve for the Images Kodak1-Kodak4	28
4.3	Images Kodak 6 (left), where the algorithms best performed, and Kodak 9 (right), the worst performing, side-by-side	30
4.4	Average ERG vs Number of JPEG Evaluations.....	33
4.5	Image Kodak17 compressed with quantization table optimization (left) vs Image Kodak17 compressed with the vanilla quantization tables (right) for the same rate	35
4.6	Image Kodak3 compressed with quantization table optimization (left) vs Image Kodak3 compressed with the vanilla quantization tables (right) for the same rate	36
4.7	Average Luminance Quantization Coefficients Values vs Transformed Coefficients in Zigzag Scan Order for the Kodak dataset with quality factor 50: Solid bars represent the average values, while error bars marks the excursion range, connecting the maximal and the minimal assumed values	37

4.8	Average Chrominance Quantization Coefficients Values vs Transformed Coefficients in Zigzag Scan Order for the Kodak dataset with quality factor 50: Solid bars represent the average values, while error bars marks the excursion range, connecting the maximal and the minimal assumed values	38
A.1	Rate-Distortion Curve for the Images Kodak5-Kodak8.....	48
A.2	Rate-Distortion Curve for the Images Kodak9-Kodak12	49
A.3	Rate-Distortion Curve for the Images Kodak13-Kodak16.....	50
A.4	Rate-Distortion Curve for the Images Kodak17-Kodak20.....	51
A.5	Rate-Distortion Curve for the Images Kodak21-Kodak24.....	52

LIST OF TABLES

2.1	Luminance quantization table	11
2.2	Chrominance quantization table	11
4.1	Bjøntegaard Delta Metric Values for Each Image (the baseline is the Baseline JPEG).....	31
4.2	Average Bjøntegaard Delta values for each approach (the baseline is the Baseline JPEG)	32
4.3	Pairwise T-Test for the BD Rates of Proposed Algorithms (the baseline is the Baseline JPEG)	32
4.4	Average Performance of a Fixed Time Compression on Kodak Dataset for Quality Factor = 75: Compression and PSNR Gains measured as the average gain across the dataset in comparison with the Baseline JPEG	34

1

INTRODUCTION AND RELATED WORK

In this chapter, an overview of the underlying problem that this work tries to address is provided and its relevance is highlighted. Related work are also scrutinized and discussed in-depth, allowing us to point out the differences and similarities between our and their works.

1.1 INTRODUCTION

In the last 25 years, the JPEG has managed to keep its position as the dominating image compression standard in the world, being widely adopted [2, 3, 4]. This success, however, was not unexpected, since the JPEG was designed from its very beginning to be a versatile state-of-the-art image compression procedure that can be performed with a tolerable computational resources consumption [5].

The wide adoption of JPEG, combined with its computationally tolerable design that shrinks the processing costs, has propelled the embrace and spread of JPEG hardware accelerators for virtually every device [4]. Since existing products usually do not get any kind of hardware enhancements or new features, they give JPEG a significative head start against any new competitor in terms of compression and decompression speed, making it barely unfeasible to simultaneously match JPEG's performance in terms of both speed and compression.

Although one can argue that an improved compression standard can lead to dedicated hardware implementations in newer devices, it is easy to notice that it would take a lot of time to achieve the level of market penetration that JPEG currently has. Moreover, during the transition time where JPEG and a new proposed standard co-exists, a lot of compatibility issues could arise.

Therefore, it is reasonable to assume that developing modifications on the top of the existing JPEG, not only guaranteeing backward compatibility but also being able to take advantage of the existing hardware and the widespread adoption of JPEG, is more promising than developing a completely new standard. In this regard, a lot of research has been conducted, dissecting approaches to minimize the perception of JPEG compression artifacts [6] in the compressed images, to optimize the entropy coding stage [7, 8], to enhance the image perception based on human visual system traits [9, 10] and, mainly, to optimize the design of the quantization tables [11, 12, 13, 14].

Due both to the broad range of applications and to the superior performance, optimizing the design of the quantization tables established itself as the leading JPEG optimization approach.

In mathematical terms, finding a quantization table that leads to a better rate-distortion compromise can be seen as an elementary optimization problem. Furthermore, since there is an implicit trade-off between the rate — or, in other words, the size of the compressed file — and the amount of distortion introduced in the image, it is a multi-objective optimization problem.

Moreover, since a quantization stage occurs in JPEG, which involves a non-analytic rounding process, the relation between the input (the original image) and the output (the compressed image) in a JPEG codec can be represented as a non-smooth, non-convex surface. This represents a family of functions well known for being hard to optimize using classical methods, such as gradient descent [15].

Nature-inspired meta-heuristics are particularly successful in handling this family of problems [16, 17], and, therefore, arises as a promising alternative to approach the quantization table optimization [14, 18].

In this work, two of the most prominent nature-inspired heuristics, Particle Swarm Optimization (PSO) [19] and Dual Simulated Annealing (DSA) [20], are employed to find the best rate-distortion compromise when generating a custom quantization table for JPEG compressing an image.

As the JPEG standard has support to custom quantization tables, the product of this process is an optimized, but still JPEG compliant image, as the standard natively incorporates support for custom tables. The quantization tables designed by this approach have created files 10% smaller than the vanilla JPEG tables for the same quality images.

1.2 RELATED WORK

A lot of research has been done investigating the customization of quantization tables in JPEG. *Chao et al.* [11] have proposed a mathematical scaling in the quantization table to improve feature repeatability in computational vision problems, mitigating the effects of compression artifacts in low rates. On the other hand, *Onnasch et al.* [21] saw the same idea as a suitable approach to enhance the quality of compressed angiographic images, while *Edmundson and Schaefer* [12] have developed a way to exploit the JPEG compression schema to improve image retrieval and indexing capabilities.

Most of the works focusing on designing custom quantization tables, however, aim to reduce the size of the compressed files or to increase the perceptual image quality of the compressed image. In this direction, nature-inspired meta-heuristics have been the dominant approaches for years [14, 18].

Costa and Veiga [22] have proposed a genetic algorithm-based approach to generate cus-

tom quantization tables, managing to slightly outperform the baseline JPEG. On its turn, *Tuba and Bacanin* [23] have employed the firefly algorithm to generate a custom quantization table for a single greyscale image, obtaining promising results, while *Tuba et al.* [24] succeeded in applying the Guided Fireworks Algorithm to optimize the quantization table for low-quality greyscale images, obtaining significative performance enhancements.

Kumar and Karpagam [25] have presented a Differential Evolution based to optimize quantization tables for greyscale images, suggesting that this approach outperforms a genetic algorithm-based approach in the same scenario. Meanwhile, *Kumar et al.* [26] have tried to generate custom quantization tables from a real coded quantum genetic algorithm, obtaining modest results, but still overtopping the baseline JPEG.

Of the two of our intended approaches, Particle Swarm Optimization was the most explored in the literature, being widely adopted to design custom quantization tables to improve the quality of hidden messages in steganography [27, 28, 29, 30]. *Ma and Zhang* present one of the most interesting results of PSO application for quantization table design, applying a cultural variant of PSO to find a Pareto front of candidates to quantization tables, being able to propose, in a single run, multiple operation points, which is very interesting and flexible, since, in contrast to the usual optimization methods, it can provide very fine-grained choices of operation points. Equally interesting is *Abbood's* [31] take on the problem, employing PSO to generate quantization tables that minimize directly the compressed image distortion, claiming to have achieved state-of-the-art results despite no information about image rates are provided. It is not worthy that, albeit similar, these works are slightly different of our proposed approach, since we aim to generate custom, image-specific quantization tables.

Regardless the fact that there is no mention to Dual Simulated Annealing applications to JPEG quantization table optimization, the vanilla Simulated Annealing was recently tested to this end by *Hopkins et al.* [32], being applied trained on a full image dataset to generate offline quantization tables for different desired qualities, considerably outperforming JPEG's vanilla tables. However, this method does not address the generation of image-specific, custom quantization tables, thus, being unable to take advantage of intra-image properties.

2 THEORETICAL FRAMEWORK

In addition to introducing and discussing in depth the fundamental concepts that are deployed in this work, from digital images and compression standards to numerical optimization meta-heuristics, this chapter establishes the adopted conventions, thus, providing us with a consistent set of definitions that guide this work.

2.1 DIGITAL IMAGE REPRESENTATION



Figure 2.1 – An Example of a Digital Image [1]

Due to the discrete nature of the digital medium, the digital representations of images must be defined as a two-dimensional function $A = f(x, y)$ [33], where x and y are the spatial coordinates of the image and A is its amplitude, a finite and discrete value that usually represents some kind of color encoding.

Usually, for gray images, a single value of amplitude, labeled gray level, is required, while for colored images generally require at least three values of amplitude, denominated channels, to describe its colors [33].

2.1.1 Color Spaces

The number of different colors that can be represented in a digital image representation is, due to its nature, discrete and, in a finite-precision, finite-channels scenario, is also finite.

Therefore, a mapping between the digital representation of the colors and the true, physical colors is needed. This mapping, that is usually required to be such as it guarantees that the distance between two colors is related to its perceptual distance and each color is clearly defined [34, 35], delimits the so-called color space, establishing a fixed number of specific colors.

2.1.1.1 RGB Color Spaces

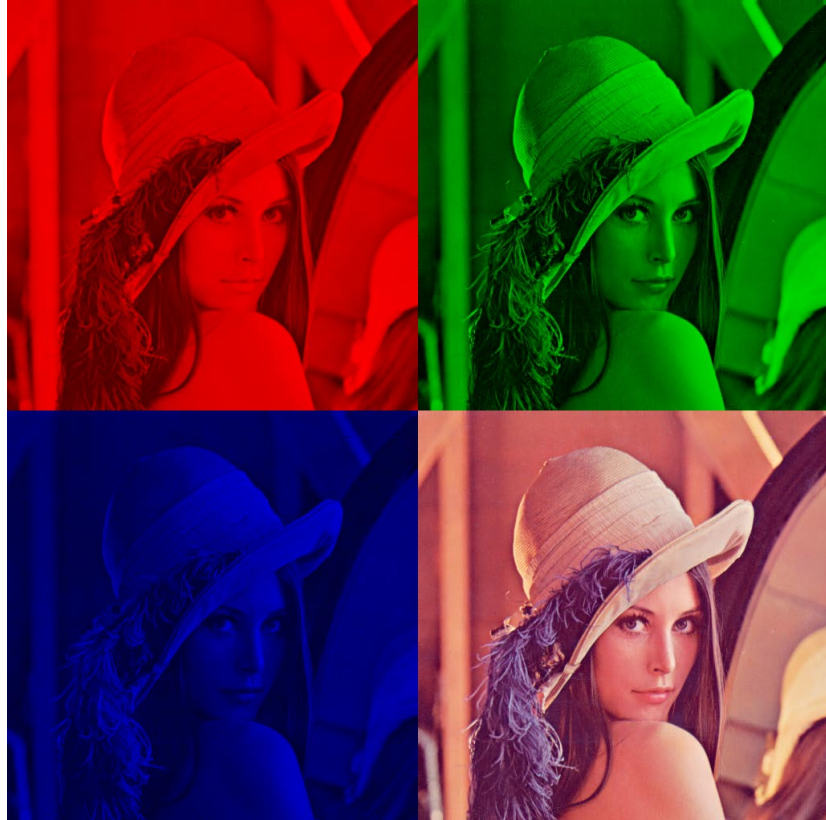


Figure 2.2 – A RGB image can be decomposed on three channels or bands: a red, a green and a blue

The RGB color Space is an additive color space based on representing human perceptible colors as a composition of red, green and blue lights [36],

The RGB color Space is often employed for representing digital images, with each amplitude A of the function $f(x, y)$ corresponding to a tuple (R, G, B) . One particularly interesting aspect of this representation is that, due to its additivity, any RGB image can be seen as the overlap of three monochromatic images, a red, defined as $f(x, y) = R$, a green, defined by $f(x, y) = G$ and a blue one, $f(x, y) = B$ [33].

Moreover, the digital representation of images using the RGB color Space also introduces the notion of bit depth. Since each color can be represented as a combination of different proportions of red, green, and blue lights, to make it compatible with a fixed-size floating-

point representation, a quantization step is needed. The number of quantization levels chosen is often defined to match the maximum representable value in the available fixed precision size. The chosen fixed precision size is called the bit depth and determines the number of different colors that can be represented in an RGB color space [37].

2.1.1.2 YC_bC_r Color Space



Figure 2.3 – Decomposition of a colored Image (upper left) into its YC_bC_r channels, the luminance (upper right) and the C_b and C_r chrominance (lower left and right) components

On the other hand, the YC_bC_r color space is a color space conceived to address characteristics of image perception by the human visual system, describing the image in terms of its achromatic information, the luma, Y , — representing the brightness of the image — and the color information denominated chroma and represented by two color-different components, C_b and C_r [36].

This representation is particularly advantageous in the context of image compression since it enables us to take advantage of the fact that the human eye is more sensitive to luminance than to chrominance, allowing us to discard some of the color information, reducing the image file size while provoking just a minor loss in the visual quality of the image, in a procedure denominated chroma subsampling [38].

2.1.1.3 Color Space Conversion

RGB images can always, with a small loss due to rounding, be converted to the $YCrCb$ color space and vice-versa. For a 8-bit representation, the conversion can be performed according to equations 2.1 and 2.2, provided by the International Telecommunication Union (ITU) [39].

$$\begin{bmatrix} Y \\ C_b \\ C_r \end{bmatrix} = \begin{bmatrix} 0.299 & 0.587 & 0.144 \\ -0.168736 & -0.331264 & 0.5 \\ 0.5 & -0.418688 & -0.081312 \end{bmatrix} \cdot \begin{bmatrix} R \\ G \\ B \end{bmatrix} + \begin{bmatrix} 0 \\ 128 \\ 128 \end{bmatrix} \quad (2.1)$$

$$\begin{bmatrix} R \\ G \\ B \end{bmatrix} = \begin{bmatrix} 1 & 0 & 1.402 \\ 1 & -0.34414 & -0.71414 \\ 1 & 1.772 & 0 \end{bmatrix} \cdot \begin{bmatrix} Y \\ C_r \\ C_b \end{bmatrix} + \begin{bmatrix} -179.5 \\ 135.5 \\ -216.8 \end{bmatrix} \quad (2.2)$$

2.2 IMAGE COMPRESSION

While the digital image representation conventions may be intuitive and even physically desirable — since colored images are rendered as the overlap of three monochromatic images —, this representation may be not efficient in terms of storage, which can be a major concern, as pictures and videos can respond for up to 80% of internet traffic [40].

Therefore, multiple techniques were developed to produce a storage-optimized representation, most of them lying in the fact that no matter how the image is represented, if any (mathematical, algorithmic) deterministic relationship can be established between the storage-optimized representation and one of the conventional representations, the image can still be rendered [41].

For generating these storage-optimized representations, in a process called image compression, two-family of approaches have stood up as dominants: compression processes where it is possible to perfectly reconstruct the original image representation $f(x, y)$, which are called lossless compression, and compression process in which it is possible to reconstruct only an approximated version $\tilde{f}(x, y)$ of the original image $f(x, y)$, establishing the so-called lossy compression processes.

Formally, we can define a lossless compression process C if there is an inverse compression process — or decompression process — C^{-1} such as equation 2.3 holds:

$$C^{-1}(C(f(x, y))) = f(x, y) \quad (2.3)$$

On the other hand, we can analogously define a lossless compression process C as a process for which there is no inverse compression process C^{-1} such as equation 2.3 holds, or, alternatively, as a compression process C such that, for any decompression process D , equation 2.4 holds:

$$D(C(f(x, y))) \neq f(x, y) \quad (2.4)$$

2.2.1 The JPEG Still Picture Compression Standard

Among many standards for image compression, the JPEG standard [42, 43] has stood the test of time, remaining for more than 25 years as both the most widely adopted image compression standard and the most used image format in the world [2, 3, 4].

This compression standard, developed by the Joint Photographic Experts Group, was meant to define a state-of-the-art, universal, and computationally feasible approach for image compression [44].

Despite a baseline codec is provided by JPEG, only the decoder is standardized and any image that can be decoded by a JPEG decoder is said to adhere to have the JPEG file format.

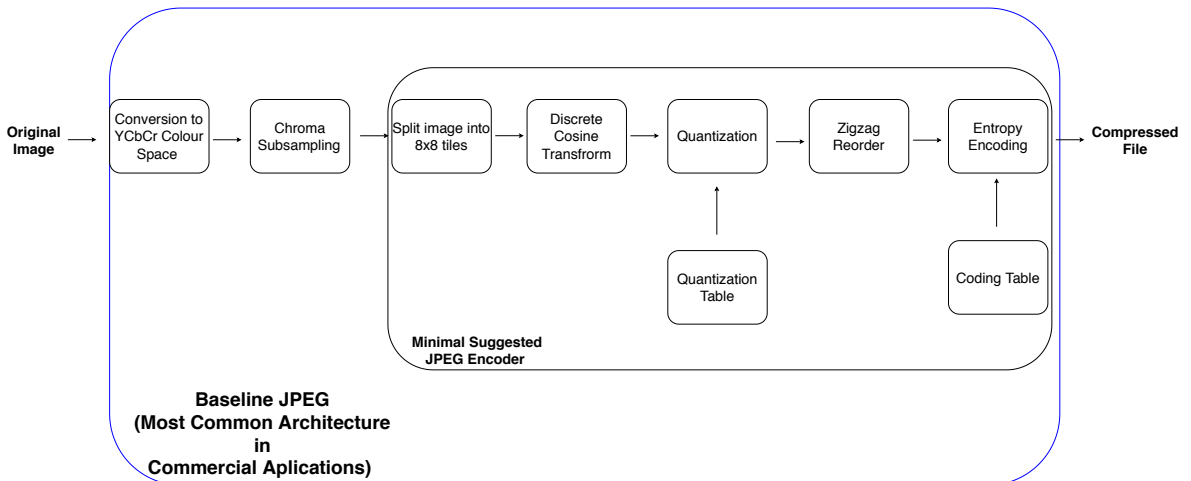


Figure 2.4 – A Block Diagram representation of the JPEG Encoding Process

For the encoding stage, the JPEG baseline architecture proposes the following steps: First, the original image is split into monochromatic 8×8 blocks — for colored image compression, each channel can be treated as a separated image —, then an 8×8 Forward Discrete Cosine Transform (FDCT) is applied in each block, being followed by a quantization step where each of the 64 coefficients of the FDCT is divided by a user-provided quantization table and rounded to the nearest integer — it is noteworthy that, since quantization is a one-to-many mapping, this is the lossy stage of the JPEG compression process, therefore, if lossless compression is intended, an all one quantization table must be employed. In sequence, the

quantized coefficients are rearranged in an alternate order, according to a procedure called zigzag scan, as illustrated in the figure 2.6, and then submitted to entropy coding, generating the compressed image [42, 43].

To foster innovation and competition among JPEG encoders, no unique FDCT algorithm implementation or fixed quantization table is defined, giving flexibility and freedom for the JPEG encoders, as long as they still produce a JPEG compliant bitstream.

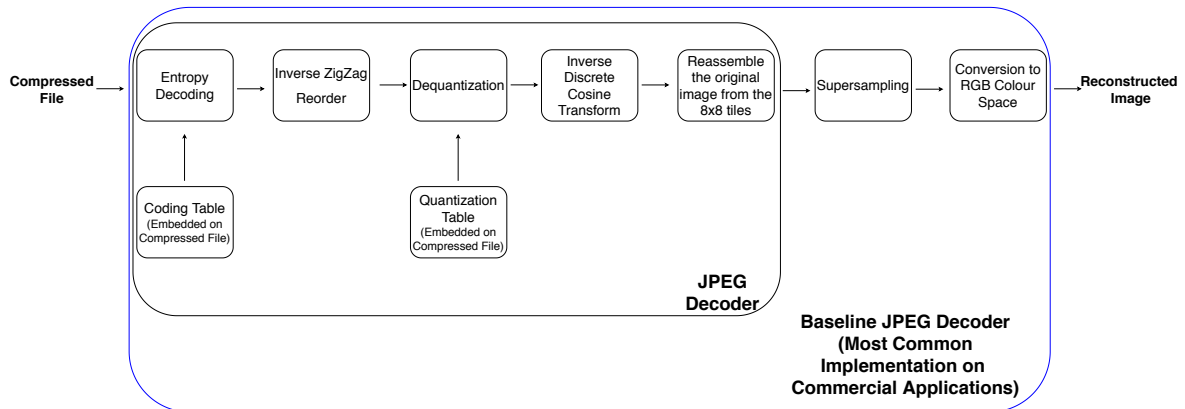


Figure 2.5 – A Block Diagram representation of the JPEG Decoding Process

On the other hand, the baseline decoder mimics the encoder behavior in inverse order, starting by decoding the compressed image, recovering zig-zag-ordered quantized FDCT coefficients, which, on its turn, are reordered and then de-quantized by the same quantization table used on the encoding — which is transmitted to the decoder as side information on the JPEG file header. Then, an inverse forward discrete cosine transform (IDFT) is applied to the resulting blocks and the recovered image blocks are reassembled into the original image size.

Since the JPEG compression standard defines a universal process for data compression, instead of a specific procedure for images with certain features, it does not define a mandatory color space for the JPEG compression and, therefore, the color space of the compressed image is the same as the original one. As chroma subsampling is also a lossy method that also provides considerable compression gains, it is widely used alongside the JPEG compression. For this reason, chroma subsampling is already incorporated by default in some JPEG codecs. In these codecs, an additional color space conversion step is necessary both on the encoder — usually, an RGB to YC_rC_b conversion — and on the decoder — analogously, a YC_rC_b to RGB conversion.

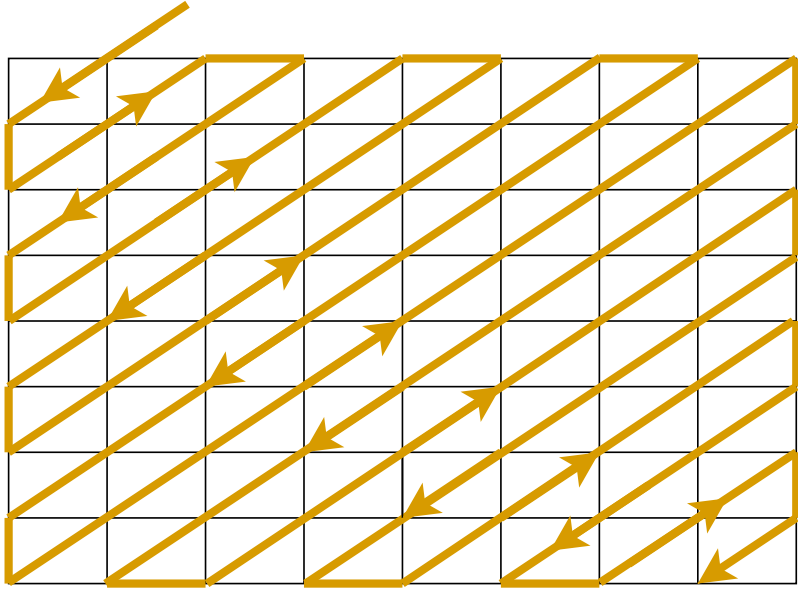


Figure 2.6 – The Zig-Zag Scan Order

2.2.2 JPEG Quantization Table

As the quantization stage is the actual lossy process in the JPEG codec, defining an appropriate quantization table is paramount. Each value in the quantization table defines the number of values that will be mapped to the same quantization level for the DCT coefficient that occupies its same position on the 8×8 DCT-transformed block. Hence, higher numbers imply lower image quality (more distortion), while smaller numbers guarantee a higher image quality (less distortion).

Although the JPEG standard does not determine a default quantization table [42], two quantization tables are provided as an example, one for luminance quantization, presented as table 2.1, and other for chrominance quantization, shown as table 2.2, are usually treated as the default quantization tables by most of commercial implementations being, therefore, referred hereinafter just as the vanilla quantization tables.

These quantization tables specify just one operation point (the combination of rate and distortion), fine-grained control of the desired image quality and image rates is usually performed through the application of a scaling factor to the whole quantization tables, which is determined from a parameter called quality factor [45]. Small quality factors indicate both low image quality and rates, while large quality factors imply high image quality and rate. The explicit relation of the quality factor, q , and the scaling factor, SF , is described in equation 2.5.

It is noteworthy that, for any 8×8 block of DCT-transformed coefficients $M = \{M_{i,j} | i, j = 1, \dots, 8\}$, and a quantization table $Qt = \{Qt_{i,j} | i, j = 1, \dots, 8\}$, the quantized block, Qm ,

16	11	10	16	124	140	151	161
12	12	14	19	126	158	160	155
14	13	16	24	140	157	169	156
14	17	22	29	151	187	180	162
18	22	37	56	168	109	103	177
24	35	55	64	181	104	113	192
49	64	78	87	103	121	120	101
72	92	95	98	112	100	103	199

Table 2.1 – Luminance quantization table

17	18	24	47	99	99	99	99
18	21	26	66	99	99	99	99
24	26	56	99	99	99	99	99
47	66	99	99	99	99	99	99
99	99	99	99	99	99	99	99
99	99	99	99	99	99	99	99
99	99	99	99	99	99	99	99
99	99	99	99	99	99	99	99

Table 2.2 – Chrominance quantization table

can be expressed according to equation 2.6. On its turn, the dequantized block, Qdm can also be trivially expressed in terms of the quantized block and the quantization table, such as specified in equation 2.7

$$SF = \begin{cases} \frac{5000}{q}, & \text{if } 1 \leq q < 50 \\ 200 - 2 \cdot q, & \text{if } 50 \leq q < 99 \\ 1, & \text{if } q = 100 \end{cases} \quad (2.5)$$

$$Qm = \{Qm_{i,j} \mid Qm_{i,j} = \left\lfloor \frac{M_{i,j}}{Qt_{i,j}} + 0.5 \right\rfloor\} \quad (2.6)$$

$$Qdm = \{Qdm_{i,j} \mid Qdm_{i,j} = Qm_{i,j} \cdot Qt_{i,j}\} \quad (2.7)$$

2.2.3 Compression Rate

The most basic compression metric to evaluate the efficiency of a compression algorithm is the Compression Rate (CR). The compression rate is a dimensionless measure defined as the ratio of the compressed image size, S_c , and the original image size, S_o as specified in

equation 2.8 [5].

$$CR = \frac{S_c}{S_0} \quad (2.8)$$

2.2.4 Image Rate

Although the compression rate works as a good and descriptive measure to assess the storage gain in the compression process, it requires information about the size of the original image file, which is not available in virtually no application out of the encoder, since the purpose of compressing an image is mostly to store or transmit only the compressed image, not transmitting it alongside with the original image.

Therefore, another approach is needed to describe the amount of compression performed on an image using just the usually available data. In this scenario, the Image Rate (R), defined as the ratio of the image file size, S , in bits, and the number of pixels in the image N_p , as presented in equation 2.9 [5].

$$R = \frac{S}{N_p} \quad (2.9)$$

Although this definition holds for any image, if the image is submitted to chroma sub-sampling it may be preferable to consider N_p not the number of pixels in the image, but the number of samples in the luminance component.

2.2.5 Mean-Squared Error

Since, in lossy compression, the compressed image, $\tilde{f}(x, y)$, is just an approximation of the original image, $f(x, y)$, it is paramount to define a way to assess how close are the two image representations. One of the most usual metrics for image similarity is the Mean Squared Error (MSE), defined as the mean of the squared differences between the image values, such as presented in equation 2.10 for monochromatic images [46]. Two factors make the MSE a widely used metric of error: It is a simple, global quality metric that is easy to calculate and punishes big mistakes in a more harsh way than small mistakes, which mimics our notion that one huge, perceptible mistake is worse than some tiny, barely perceptible mistakes [47].

$$MSE = \sum_{i=1}^m \sum_{j=1}^n \frac{(\tilde{f}(x_i, y_j) - f(x_i, y_j))^2}{m \cdot n} \quad (2.10)$$

While equation 2.10 single-handedly defines the MSE for monochromatic images, there is no convention on how to calculate the MSE for colored images [48]. In this work, the MSE for a multichannel image with N_c channels is defined as the average of the MSEs of each channel, such as specified in equation 2.11.

$$MSE_{MC} = \sum_{k=1}^{N_c} \frac{MSE_k}{N_c} \quad (2.11)$$

2.2.5.1 Peak Signal-to-Noise Rate

Although the MSE is pretty useful and straightforward, it also suffers from some major drawbacks. Among the problems of the Mean Squared Error, we can cite that it is a squared metric, and, thus, not only being in a different scale than the pixel values but also having a huge range of possible values, which makes the MSE values hard to compare and interpret. Moreover, the MSE is a measure of error, not image quality, hence, the MSE scale only has a loose correlation with how the mistakes are perceived by an observer — i.e., if a given image has twice the MSE of other, it does not mean that the image will be perceived as twice worse —, and higher of values MSE means worse image quality, what can be a little misleading [49].

To address these problems, the PSNR (Peak Signal-to-Noise-Ratio) arises as an interesting alternative, turning the MSE into a range-constrained easily-comparable metric that correlates much better with distortion perception by the human visual system due to its logarithmic scaling [50, 51]. For a b bits image representation, the PSNR can be obtained from the MSE for a given image as described by equation 2.12.

$$PSNR = 10 \cdot \log_{10} \left(\frac{2^b - 1}{MSE} \right) \quad (2.12)$$

2.2.6 Lagrangian Rate-Distortion Cost Function

Since image compression processes are, by its nature, multi-objective optimization problems, where the main goal is to simultaneously minimize the size of the compressed image and the distortion, despite existing an inherent trade-off between these two objectives, comparing the results of two different compression processes is a hard multidimensional comparison problem, especially if the two results are Pareto non-comparable.

To simplify this problem and support decisions when the compounds are Pareto non-comparable, some sort of equivalence between the size of the compressed image, in general, expressed as the Image Rate, and the distortion, usually expressed in terms of the Mean

Squared Error, must be established.

A classical formulation that allows us to simultaneously minimize the image rate and the distortion is to minimize the sum of the distortion and the image rate, scaled by an exchange factor relating rate and distortion. This formulation resembles the notion of Lagrange multipliers, with our arbitrarily defined rate-distortion exchange factor working as a Lagrange multiplier [52, 53]. Therefore, this formulation is called Lagrangian Cost Function, defined as follows in equation 2.13:

$$CF = MSE + \lambda R \quad (2.13)$$

Where CF is the Lagrangian Cost Function, MSE is the mean squared error, λ is a Lagrange multiplier relating image distortion and rate and R is the image rate, in bits per pixel.

2.2.7 Bjøntegaard Delta Metric

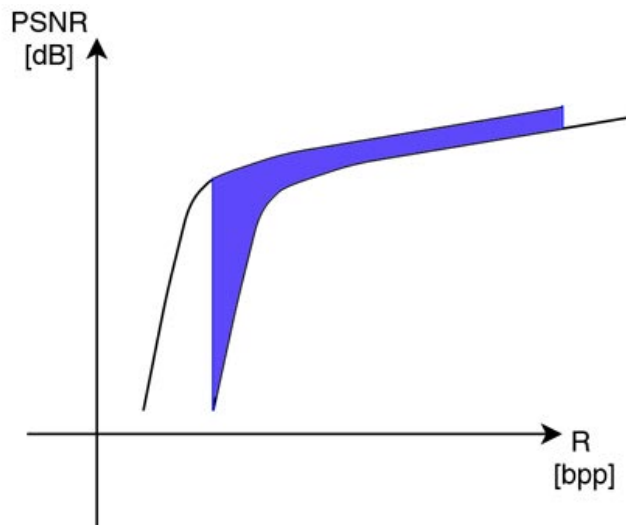


Figure 2.7 – Two rate-distortion curves represented in the same figure: The Bjøntegaard Delta is numerically equivalent to the filled area

While the Lagrangian Cost Function is useful to make point-wise rate-distortion comparisons, it cannot be applied to compare the performance of rate-distortion curves.

In this context, the Bjøntegaard Delta raises as an alternative approach to compare different rate-distortion curves [54]. Assuming that a rate-distortion curve, T can be defined from an rate-ordered arbitrary set of N experimental rate-distortion points $(R, PSNR)$, $T = \{(R_i, PSNR_i) | R_i < R_{i+1} \wedge i = 1, \dots, N\}$, and defining $Q_1(R)$ and $Q_2(R)$ as the functions that describes the $PSNR$ for a rate R interpolated from two sets of experimental points T_1 and T_2 , we can define the Bjøntegaard Delta for PSNR, $BD - PSNR$, with equation 2.14, it is, as the area between the curves Q_1 and Q_2 between range defined by the

overlapping range for the two curves, in order to avoid extrapolations.

$$BD - PSNR = \int_{\max(R_{1,1}, R_{2,1})}^{\min(R_{1,N_1}, R_{2,N_2})} Q_2(R) - Q_1(R) \quad dR \quad (2.14)$$

Analogously, a Bjøntegaard Delta for Rates, $BD - RATE$ can also be defined, changing the limits of integration to the overlapping range of PSNRs and the rate-distortion curve Q for its inverse Q^{-1} , where $(Q^{-1} \circ Q)(R) = R$, as presented in equation 2.15.

$$BD - PSNR = \int_{\max(PSNR_{1,1}, PSNR_{2,1})}^{\min(PSNR_{1,N_1}, PSNR_{2,N_2})} Q_2^{-1}(PSNR) - Q_1^{-1}(PSNR) \quad dPSNR \quad (2.15)$$

2.3 NUMERICAL OPTIMIZATION

Maximization and minimization problems are very common both in theoretical and practical grounds. But although these problems can be easily solved in two-dimensions if a closed-form expression is provided, they can become quite challenging in manifolds or even if it is intended to optimize a data generating process that cannot be expressed in an analytic form.

Even though it is not an easy task, determining the best possible solution according to a given criteria continues to attract a lot of interest, with many numerical approaches been developed to find computationally, in a reasonable amount of time, an approximated solution to the optimization problem, regardless of the number of dimensions of the problem, the existence of local minima and maxima and the analyticity of the data generating process.

To overcome the curse of dimensionality, numerical optimization methods are often stochastic rather than deterministic, introducing, thus, an exploratory capability that helps these methods to avoid getting stuck in a local optimum, while output dependent only algorithms with non-parametric update rules are the usual take to cope with non-analytic data generating processes.

This work heavily deploys two of these methods, namely Particle Swarm Optimization and Dual Simulated Annealing, to optimize JPEG's quantization tables, such as the compressed image has a better rate-distortion compromise than the images generated by the JPEG default quantization tables.

2.3.1 Particle Swarm Optimization (PSO)

The Particle Swarm Optimization is a derivative-free, population-based meta-heuristic that was originally intended to simulate the behavior of a flock of birds [55]. Like a bird in a bird flock or a fish in a school of fish, a particle in a particle swarm both benefits from and helps to builds social knowledge, allowing the entire swarm's to converge to the best position [56] - i.e, the position that maximizes a given reward, such as the survival chance for a bird flock or an objective function for PSO.

In mathematical terms, PSO can be seen as an optimization method where candidate solutions, called particles, sweep out a n -dimensional search space, varying their position vector, X , in each iteration, t , according to an stochastic parameter vector called velocity, V , influenced both by particle's, P , and swarm's, G , best known position [19, 57, 58], according to the following update rules:

$$\begin{aligned} V_i^{t+1} &= C_0 V_i^t + C_1 R_1 (P_i - X_i^t) + C_2 R_2 (G - X_i^t) \\ X_i^{t+1} &= X_i^t + V_i^{t+1} \end{aligned} \quad (2.16)$$

where R_1 and R_2 are random values sampled from a uniform distribution, and C_0 , C_1 and C_2 are constants.

From this formulation, it is very neat the that parameters C_0 , C_1 and C_2 control both how much the previous velocity, the particle's best-known position and the swarm's best know position influence in the velocity update and how much the updated velocity influences in the position update. Moreover, the random factors, R_1 and R_2 secures the stochastic behavior of the algorithm, warranting that to the algorithm some level of robustness to local optima traps.

The convergence in PSO seems to be promoted by the fact that particles do not move freely, but instead are continuously attracted to particle's and swarm's best known positions by the terms $C_1 R_1 (P_i - X_i^t)$ and $C_2 R_2 (G - X_i^t)$ in equation 2.16 [59]. To avoid the velocity to grow or decay unbounded in any dimension, a non-required, but still useful pair of parameters V_{max} and V_{min} are often set, so the velocity can be clipped, improving the stability of the method [60]. The same logic can be applied to the position, if it is intended to keep the positions confined to a sub-space, i.e. in a restricted optimization problem.

While hyper-parameter tuning is still critic in PSO and it has been shown to have considerable influence on PSO's performance [61, 62, 63], it still does have fewer parameters to tune than its competitors and the PSO hyper-parameter tuning is a widely discussed problem [64].

2.3.2 Dual Simulated Annealing (SA)

The Dual Simulated Annealing (SA) is a stochastic global optimization metaheuristic [20], combining Classical [65] and Fast Simulated Annealing [66] with local search improvements [67]. The idea of SA is to emulate the process of internal energy minimization in physical systems.

Therefore, in each iteration, a random point is chosen, drawn from a probability distribution where the probability decreases as the distance from the current point increases, and its fitness is evaluated. If the new point has better fitness than the current point, it becomes the next point. Else, it has a small probability to become the next point. This probability is called the acceptance probability of a transition and is determined both by the fitness values of the current and the new, random position and by a time-varying, hyper-parameter called Temperature, which controls the operation point of the exploration-exploitation by adjusting the tendency of the algorithm to accept uphill moves. This stochastic decision is precisely what enables the algorithm to escape from local optima traps.

By default, the Temperature parameter is lowered after each iteration, usually in a hyperbolic decay, reducing the search range and, therefore, converging to global optima.

A usual choice for the transition acceptance probability function is the Cauchy-Lorentz visiting distribution, as extensively discussed in [68] and [69].

On the other hand, the Temperature parameter T_q , in the t -th iteration can be determined by equation 2.17, as following:

$$T_q(t) = T_q(1) \cdot \frac{2^{q-1} - 1}{(1 + t)^{q-1} - 1} \quad (2.17)$$

where the parameter q is the shape controller parameter of the Cauchy-Lorentz visiting distribution.

The transition acceptance probability, p_a , can be derived from a generalized Metropolis algorithm and calculated from the difference between the fitness values in the new point and the current point, ΔE , the Metropolis–Hastings acceptance rate, β , and the Cauchy-Lorentz shape controller parameter, q , according to equation 2.18:

$$p_a = \min\{1, \max\{[1 - (1 - q)\beta\Delta E]^{\frac{1}{1-q}}, 0\}\} \quad (2.18)$$

3 METHODOLOGY

In this work, two nature-inspired meta-heuristic based methods for generating image-specific, rate-distortion optimized quantization tables in JPEG compression are proposed and evaluated. The main advantage of this approach is that the compression process is built on the top of JPEG, thus, not only benefiting from the widespread availability of dedicated hardware available but also guaranteeing that the produced image will be JPEG compliant, having its custom quantization table embedded on the file bitstream, as specified by the JPEG standard [42].

3.1 QUANTIZATION TABLE OPTIMIZATION

A high-level overview of nature-inspired meta-heuristic for optimization describes a very straight-forward procedural behavior: A population of candidate solutions is initialized and each candidate solution is evaluated according to a given fitness function and the population is updated according to a set of pre-established algorithmic rules. This process continues until the algorithm reaches a stop criteria, usually, a fixed number of maximum allowed iterations or a fixed amount of tolerable error or a needed update.

Therefore, any application of PSO or DSA to optimize quantization table must handle three main issues: i) representing the candidate solutions, it is, the quantization tables, in a format that is compatible with the algorithm's update rules; ii) determining how to initialize the initial population; and iii) defining how to evaluate the quality of a solution, establishing, for this purpose, a proper fitness function.

Once these three issues are solved, both PSO and DSA can run unobstructedly to optimize the quantization tables, initializing the population, representing each candidate solution, as defined, evaluating each solution according to the provided fitness function and updating it observing algorithm's own rules, in an iterative process that lasts until a stop criterion is met.

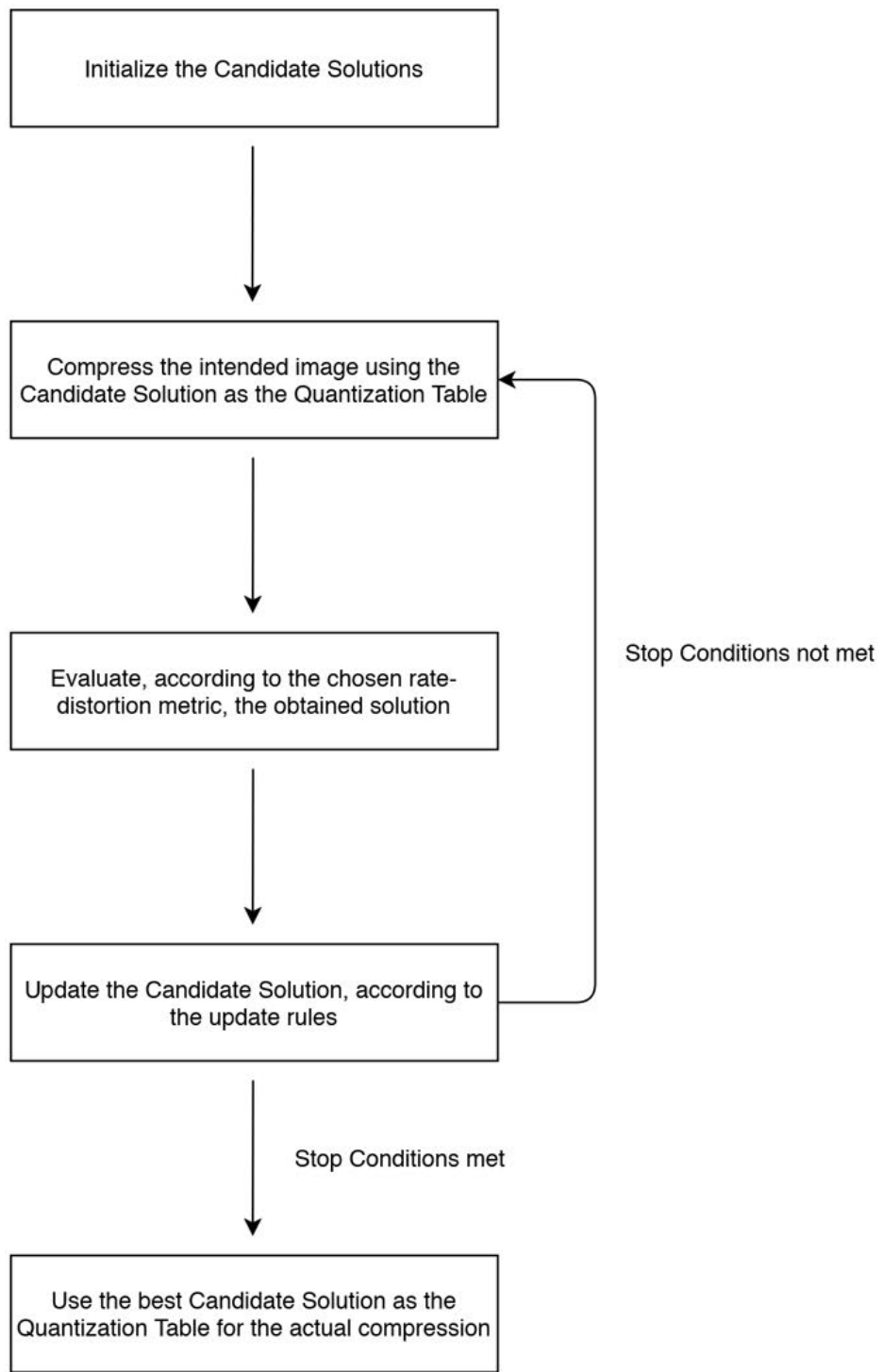


Figure 3.1 – Fluxogram of the nature inspired metaheuristic behaviour on optimizing JPEG quantization tables

3.2 QUANTIZATION TABLE REPRESENTATION

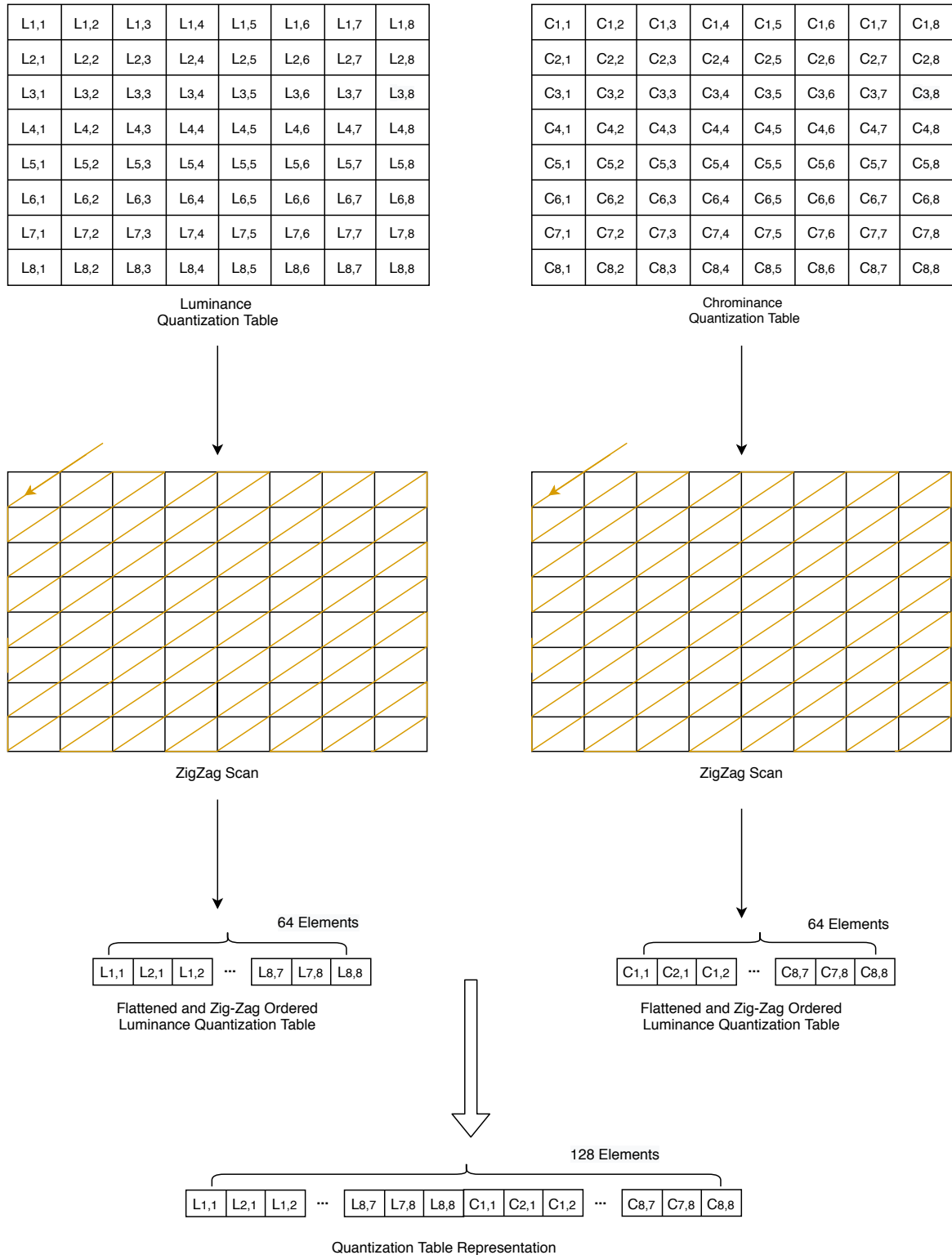


Figure 3.2 – Quantization Table Pre-Processing Process

The JPEG standard [42] does not define a default quantization table, but rather establishes that the chosen quantization tables must be informed to the decoder, by embedding it, in a

specified format, as side information on JPEG’s bitstream. Despite this, most of the commercial encoders use the vanilla quantization tables for luminance and chrominance, presented in tables 2.1 and 2.2, as their default quantization tables, scaled by the quantization factor.

To benefit from the commercial implementations of JPEG, which usually convert the images to the YC_bC_r color space and apply chroma sub-sample before compressing the image, different quantization tables will also be deployed to quantize luminance and chrominance. Therefore, a representation able to wrap both quantization tables, as a pair, as a single candidate solution compatible with PSO and DSA update rules is needed.

Since both PSO’s and DSA’s update rules lie upon linear operations, a possible way to represent our quantization table pair is defining each candidate solution as a 128-dimensions vector, where the first 64 dimensions correspond to the luminance quantization table coefficients, while the last 64 are the chrominance quantization table coefficients.

Mathematically, for luminance quantization table coefficients $Ql = \{Ql_i \mid 1 \leq i \leq 64\}$, and chrominance quantization table coefficients $Qc = \{Qc_i \mid 1 \leq i \leq 64\}$, both arranged in any reversible order, we can assemble a candidate solution vector, $X = \{X_i \mid 1 \leq i \leq 128\}$, such as:

$$X_i = \begin{cases} Ql_i, & \text{if } 1 \leq i \leq 64 \\ Qc_{i-64}, & \text{if } 64 < i \leq 128 \end{cases} \quad (3.1)$$

3.3 INITIAL GUESS

Despite being global optimization methods, both Particle Swarm Optimization and Dual Simulated Annealing are stochastic by nature, which means that there is no theoretical guarantee they will converge to the global optima in a finite amount of time. For this reason, providing a good initial guess plays an important role to speed up the convergence of the algorithm or even guaranteeing that eventual sub-optimal solutions are still useful.

One may argue that the very notion of quality factor is, indeed, somehow an initial guess heuristic on its own, since, rather than having to determine and explicitly provide a quantization table able to produce an image that meets the expected quality criteria, only the quality factor, which is directly related to the desired image quality and image rate.

Thus, a promising initialization heuristic is to define the initial population as a variation of the vanilla quantization table derived from the intended quality factor. If no quality factor, but rather a target image rate or quality is provided, the correspondent quality factor can be found iteratively or even by the application of a simple classic genetic algorithm.

For a initial population P , composed of N candidate solutions P_i , such as $P = \{P_{i,j} \mid 1 \leq$

$i \leq N$ $1 \leq j \leq 128\}$, assuming that the vectorial representation of the vanilla quantization table scaled by a quality factor q is given by $X^q = \{X_i^q \mid 1 \leq i \leq 128\}$, our population can be initialized according to the equation 3.2.

$$Cs_j = X_j^q + R(-\gamma, \gamma) \quad (3.2)$$

$$P_{i,j} = \begin{cases} Cs_j, & \text{if } 1 \leq Cs_j \leq 255 \\ 255, & \text{if } Cs_j = 255 \\ 0, & \text{if } Cs_j < 1 \end{cases}$$

Where $R(-\gamma, \gamma)$ is a random number drawn from a uniform discrete distribution with boundaries $[-\gamma, \gamma]$. In this work, a value of $\gamma = 20$ was arbitrarily assumed to reasonably limit the spread of the initial population in the search space.

3.4 FITNESS FUNCTIONS

Establishing a proper metric to evaluate the quality of the proposed solutions is a must for obtaining a good performance in the optimization processes, regardless of the chosen optimization methods. And although this assumption still holds, the choice of the evaluation metrics impact on Particle Swarm Optimization and Dual Simulated Annealing is quite different.

As Particle Swarm Optimization update rules do not lie in the fitness value, but rather only in determining which solution is the best among a set of given solutions, it presents relative robustness to how a fitness function grades the quality of the candidate solutions, that is, PSO only uses information about what is the best solution, and do not take in consideration how good (or how better than the last best solution) is the best solution when updating its candidate solutions.

On the other hand, Dual Simulated Annealing update rules have a strong dependence on the fitness value, emphasizing the importance of the choice of a proper fitness function, since the probability of accepting a transition is a function of the difference of the current candidate solution and the proposed candidate solution fitness values.

Usually, the fitness function works as a proxy to the optimization target. Since this work aims to find a quantization table that yields a better rate-distortion compromise than the vanilla JPEG quantization tables, the classic approach in the literature is to resort to the Lagrangian rate-distortion function.

For this purpose, a new fitness function, named Fixed Quality Expected Rate Gain, is pro-

posed aiming to benefit from optimizing the rate-distortion compromise in a non-parametric, model-free fashion, and the results of quantization tables generated by optimizing the Fixed Quality Expected Rate Gain are benchmarked against the classical approach, minimizing the Lagrangian Rate-Distortion Cost Function.

3.4.1 The Fixed Quality Expected Rate Gain (FQ-ERG)

Albeit classical, the Lagrangian cost function may be argued the simplest of all fitness functions, since it establishes a static, linear exchange rate between image rate and image distortion, intrinsically assuming that a change in the image rate should produce a proportional change in the introduced distortion among all the support of possible image rates, which is mostly not true.

An alternative formulation to cope with the non-linearity in the rate-distortion relation is to assume that the rate and distortion have a fixed exchange rate just around a given operating point. The Fixed Quality Expected Rate Gain (FQ-ERG) generalizes this idea, providing a self-adaptive metric that requires very few or actual no hyper-parameter tuning.

Since we expect that there is an almost monotonic relationship between the image rate, R , usually expressed in bits per pixel, and the amount of distortion introduced, D , often described in terms of MSE or $PSNR$, the expected rate function, $E(D)$, can be defined from a linear interpolation of the rate and distortion, such as described in the equation 3.3.

$$E(D) = \text{interp}(D, R) \quad (3.3)$$

where $\text{interp}(D, R)$ correspond to the linear interpolation considering the D points as the points for the x coordinate, while the R points are the points for the y coordinate, and $E(D)$ stands for the expected rate function for a image with distortion D .

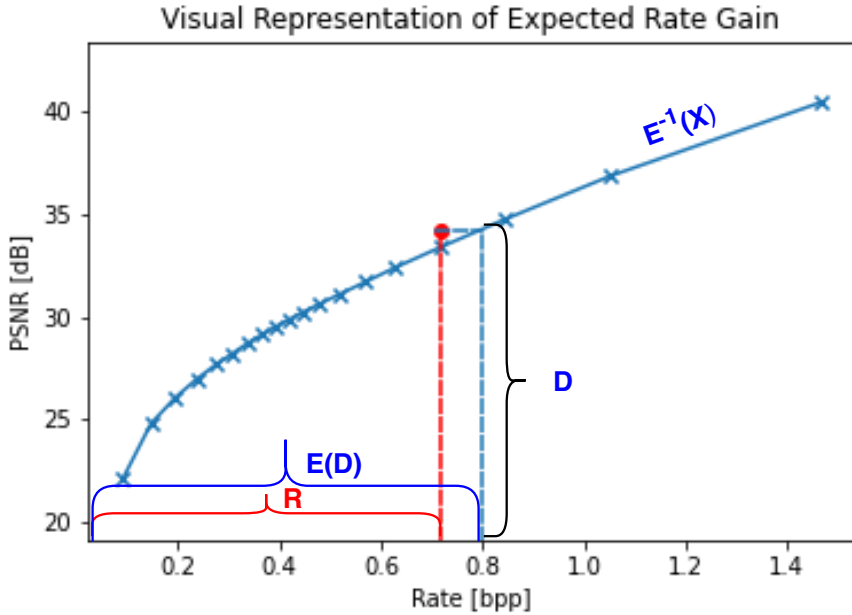


Figure 3.3 – Graphical Representation of the Expect Rate Gain for a given operation point: The ERG corresponds to the ratio between the actual point rate, R , and the projected rate to baseline JPEG produce a same quality image, $E(D)$

Knowing beforehand how rate and distortion are expected to relate to each other, we can measure the expected rate gain, ERG for a compression process that produces an image with rate R and distortion D according to the equation 3.4.

$$ERG = \frac{R}{E(D)} \quad (3.4)$$

Although the ERG manages to summarize the reduction in the compressed file size, while preserving the image quality, in a very neat way, it can be seen easily that it still cannot be directly minimized, since an attempt to minimize the ERG would incur in finding an arbitrary operation point where a custom quantization table outperforms the anchor quantization table set — it is, the set of quantization tables used to generate the (R, D) pairs used to fit the linear interpolation for the obtention of the expected rate function — by most.

While this result can be useful to propose the best compression settings when no targeted image quality is specified, in most of the usual applications, it is necessary to guarantee that the compressed image meets the image quality standard determined by the end-user and the intended application. For this reason, modifications are needed to add support to fine-grained image quality control, which finally leads us to the proposed metric, Fixed Quality Expected

Rate Gain (FQ-ERG), defined according to equation 3.5.

$$FQ - ERG = \begin{cases} ERG, & \text{if } |D - D^*| \leq \epsilon \\ ERG + |D - D^*| \cdot P, & \text{if } |D - D^*| \leq \epsilon \end{cases} \quad (3.5)$$

where D is the distortion in the compressed image, D^* is the target distortion, ϵ is the distortion tolerance range and P is a penalty factor.

With a little effort, one may realize that, for an adequate value of P , minimizing the FQ-ERG tends to have exactly the intended behavior of finding the best rate-distortion comprise within the acceptable image quality range, since every time that a candidate solution provides an image that exceeds or fails to meet the tolerable image quality standards, a penalty will be introduced and, thus, the assigned fitness value will be worse than similar performing candidate solutions that produce images in the acceptable range.

It is also noteworthy to notice that, unlike the Lagrangian Cost Function, that demands intensive hyper-parameter tuning, since the Lagrangian multiplier, λ , assumes a different value for each operation point, with a grid search often being required to determine a proper value for the intended image quality, the $FQ - ERG$ requires barely any parameter tuning since it requires only three parameters, two of which — the targeted image quality and the distortion tolerance — are known in advance, and the third, the penalty factor, has low sensitivity and, for practical effects, can be fixed as 2.

3.5 IMPLEMENTATIONS

Since the JPEG standard specifies only a decoder, leaving encoder implementations open to competition [42], the Independent JPEG Group's JPEG still image codec v9 encoder is employed [70] as our reference implementation. The encoding process in the Independent JPEG Group implementation is illustrated in figure 2.4

On the other hand, for Particle Swarm Optimization, the DEAP library [71] implementation is adopted, with the following setting of hyper-parameters:

- Population Size = 20
- Maximum Number of Generations = 50
- Maximum Local Update Factor = 2.0
- Maximum Global Update Factor = 2.0
- Minimum Speed = -3.0

- Maximum Speed = 3.0

Finally, for Dual Simulated Annealing, the Scipy implementation [72] is employed as a reference, preserving the default set of parameters, except for the maximum number of allowed function evaluations (maxfun), which is set as 1000.

4 RESULTS

In this chapter, the proposed approach is empirically validated, being evaluated in terms of performance, number of iterations and elapsed real time. The results are presented and discussed.

4.1 SETTINGS

To verify the proposed concept, both Particle Swarm Optimization and Dual Simulated Annealing were employed to generate custom, image-specific quantization tables for every image on the *Kodak Image Dataset*, presented on Fig. 4.1, a dataset composed by 24 uncompressed, 768 x 512 or 512 x 768 true color images. For each image, custom quantization tables were generated for 19 different target quality factors, ranging from $q = 5$ to $q = 95$ in steps of 5, by optimizing Fixed Quality Expected Rate Gain and the Lagrangian Cost Function. When optimizing the Lagrangian Cost Function, the value of the Lagrangian multiplier λ for each quality factor and image was determined through a grid search.



Figure 4.1 – The Kodak Image Dataset

4.2 NUMERICAL EVALUATION

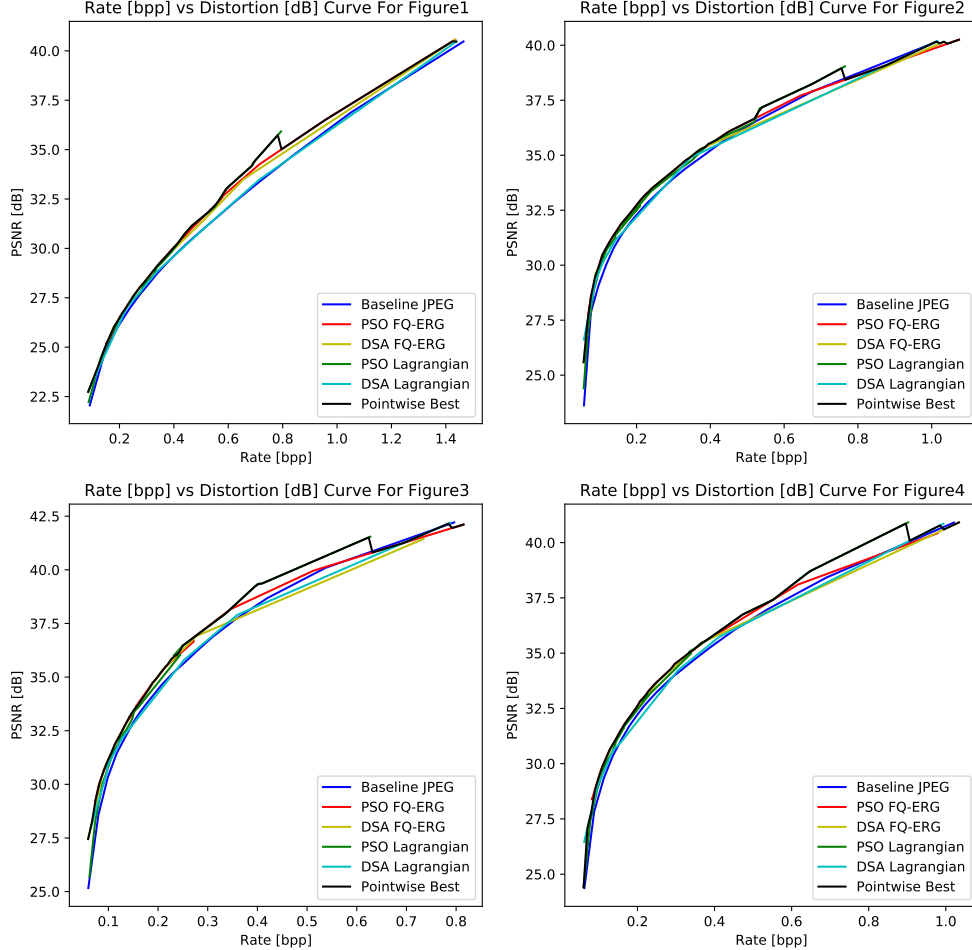


Figure 4.2 – Rate-Distortion Curve for the Images Kodak1-Kodak4

To allow consistent comparison of the proposed approaches, the image rate, in bits per pixel, and the Peak Signal-to-Noise-Ratio (PSNR), in dB, are chosen as the main rate and distortion metrics, respectively. Moreover, a complete overview is provided by presenting the rate-distortion curve and the Bjøntegaard Delta Rate and PSNR values for each image and each algorithm.

The rate-distortion curves, of which one sample is displayed in figure 4.2, while the others are presented in appendix in figures A.1 and -A.5, show us that all the proposed methods can outperform the baseline JPEG for any image rate. It is interesting to notice that, despite all methods eventually outperform the baseline JPEG, the Particle Swarm Optimization with the FQ-ERG metric triumphs in low image rates, while the Dual Simulated

Annealing with FQ-ERG stands out for medium rates. However, we may notice that, for very high image rates, the proposed methods outperform only slightly the baseline JPEG encoder, even losing in some scenarios. This behavior is more frequent when the image rates are over 1.0 bit per pixel, which is considered an adequate rate to store excellent quality images [5].

Another noteworthy observation is that the behavior of Particle Swarm Optimization generated tables is very similar, regardless of the choice of the fitness function, and is somehow smooth, while Dual Simulated Annealing performance is heavily influenced by the chosen fitness function and, in general, is much more ill-behaved. We believe these behaviors are consistent with the inner logic of the algorithms.

For the Particle Swarm Optimization, we can argue that, since its update rules do not take in account the fitness value of the best candidate solution, but only the solution itself, the algorithm has higher robustness in terms of the fitness function, since, as long as different fitness functions rule the same candidate as the best, the algorithm will perform the same update. Moreover, since it is a population-based method, the social knowledge component makes the candidate solutions to iteratively move towards the best-known solutions, guaranteeing, thus, a stable behavior.

On the other hand, the Dual Simulated Annealing high sensitivity to the choice of the fitness function can be justified by the fact that the transition acceptance probability is a function of the difference of the fitness values, hence, a change in the fitness function implies in a considerable change in the transition acceptance probability. Furthermore, it is our understanding that the noisy behavior can be explained by its overly stochastic nature since abrupt transitions are evaluated stochastically, which may lead to improbable, but substantial improvements that are hard to be replicated — for example, for a different setting or fitness function.

In terms of the Bjøntegaard Delta metric, table 4.1 describes comprehensively the results obtained per method and per image, which is summarized to enable neater comparisons in table 4.2. It is worthy to highlight that all the proposed algorithms consistently outperformed baseline JPEG and presented results around a mean, with small variation in different images, validating the idea that the proposed method is generic, do not require exploring any fixed particular (statistic) characteristic in the compressed images, rather determining, for each image, a way to use its particular characteristics to improve its compression.



Figure 4.3 – Images *Kodak 6* (left), where the algorithms best performed, and *Kodak 9* (right), the worst performing, side-by-side

We can also notice that the algorithms perform worst on image *Kodak9*, while the best performance is assured when compressing image *Kodak6*, both pictures on the water. One factor that may explain these results is that, while image *Kodak6* has large areas of similarly toned pixels, and with colors segmented — the sea corresponds to most of the turquoise of the image, while almost red, white and brown are on the boat and the green and grey are on the ground —, the image *Kodak9* is hard to segment, having very similar colors to both water and sky, worsened by the clouds and the blur in the background, while the foreground has irregularly shaped, distinctly colored sailing boats with vivid colors, also having far more color transitions — almost everywhere in the sky and in the water, since there are a lot of clouds, churning, a mountain in the background and a sail intersecting both in the foreground and even in the sail since there are very different colored regions and the sailors are wearing flashy jackets.

Another intriguing result can be brought up by analyzing in-depth the standard deviation of the BD rates of each algorithm. While the standard deviation of the BD rates for the PSOs are around 0.7, which corresponds to a coefficient of variation of about 8.5%, the DSAs have higher standard deviations — about 1.13 for the FQ-ERG DSA and 0.83 for the Lagrangian optimized DSA — and even higher coefficients of variation — 14.3% and 21.2%, respectively —, which strengthens our hypothesis that they have a less stable behavior than their PSOs counterparts, probably due to its overly stochastic formulation that allows abrupt transitions.

Table 4.2 also provides us with useful information, making explicit that the FQ-ERG provides a huge performance boost for the DSA algorithm, virtually leveling its performance

Image Name	PSO (FQ-ERG)		PSO (Lagrangian)		DSA (FQ-ERG)		DSA (Lagrangian)		Pointwise Best	
	BD Rate	BD PSNR	BD Rate	BD PSNR	BD Rate	BD PSNR	BD Rate	BD PSNR	BD Rate	BD PSNR
Kodak 1	-8.04	0.49	-8.11	0.50	-8.51	0.46	-2.97	0.21	-8.99	0.53
Kodak 2	-7.97	0.48	-8.42	0.49	-7.41	0.46	-5.18	0.44	-8.98	0.59
Kodak 3	-8.79	0.59	-9.45	0.67	-8.19	0.61	-4.29	0.35	-10.83	1.08
Kodak 4	-8.17	0.47	-8.12	0.53	-7.46	0.46	-3.99	0.33	-8.86	0.56
Kodak 5	-8.54	0.59	-8.80	0.55	-8.50	0.53	-4.46	0.29	-9.06	0.61
Kodak 6	-8.39	0.53	-8.92	0.55	-9.62	0.63	-4.08	0.25	-11.63	1.02
Kodak 7	-8.54	0.59	-9.46	1.00	-8.71	0.67	-4.23	0.33	-10.91	0.80
Kodak 8	-7.60	0.56	-7.31	0.51	-8.52	0.56	-2.51	0.19	-8.12	0.57
Kodak 9	-7.25	0.42	-8.74	0.59	-5.71	0.36	-4.04	0.25	-7.21	0.46
Kodak 10	-7.27	0.47	-8.73	0.56	-6.87	0.44	-3.83	0.29	-9.45	0.62
Kodak 11	-8.97	0.53	-8.05	0.51	-9.19	0.58	-4.35	0.26	-10.69	0.64
Kodak 12	-7.38	0.46	-8.52	0.48	-6.40	0.40	-4.75	0.31	-7.97	0.50
Kodak 13	-9.34	0.67	-6.39	0.40	-9.25	0.50	-3.06	0.17	-9.20	0.58
Kodak 14	-9.25	0.51	-8.91	0.50	-8.44	0.45	-3.88	0.22	-9.96	0.54
Kodak 15	-8.77	0.50	-7.99	0.50	-7.25	0.45	-3.84	0.28	-9.12	0.58
Kodak 16	-8.63	0.52	-8.26	0.52	-8.11	0.52	-3.75	0.24	-9.94	0.61
Kodak 17	-7.75	0.47	-9.18	0.55	-7.38	0.46	-2.87	0.17	-9.19	0.57
Kodak 18	-8.11	0.47	-7.80	0.42	-8.24	0.45	-2.12	0.12	-8.74	0.48
Kodak 19	-8.31	0.49	-8.86	0.55	-8.95	0.57	-4.57	0.30	-10.32	0.64
Kodak 20	-6.92	0.43	-6.95	0.42	-7.72	0.53	-3.41	0.22	-8.89	0.59
Kodak 21	-7.99	0.49	-8.44	0.53	-9.29	0.61	-5.01	0.32	-10.27	0.65
Kodak 22	-8.25	0.41	-8.25	0.45	-7.14	0.37	-2.94	0.16	-8.86	0.45
Kodak 23	-8.02	0.50	-8.40	0.54	-4.71	0.27	-3.95	0.25	-7.53	0.47
Kodak 24	-10.18	0.60	-9.04	0.50	-8.72	0.48	-5.71	0.32	-10.61	0.61
Average	-8.27	0.51	-8.38	0.53	-7.93	0.49	-3.91	0.26	-9.38	0.61

Table 4.1 – Bjøntegaard Delta Metric Values for Each Image (the baseline is the Baseline JPEG)

Method	BD Rate	BD PSNR
PSO FQ-ERG	-8.26	0.51
PSO Lagrangian	-8.37	0.52
DSA FQ-ERG	-7.92	0.49
DSA Lagrangian	-3.90	0.26
Pointwise Best	-9.38	0.59

Table 4.2 – Average Bjøntegaard Delta values for each approach (the baseline is the Baseline JPEG)

with the PSO. While both pure PSO approaches and DSA FQ-ERG gives us an enhancement of about 8% in the compression rate, a pointwise combination of these methods — both optimized quantization tables are independently determined and the best performing is adopted, for each operating point — can provide an additional gain of over 1%, raising the compression rate improvement to about 9.4%, despite nearly doubling the computational cost of the procedure.

It is prudent to consider that, since our benchmark was limited to our dataset, slight differences in terms of performance can occur due to randomness, and taking any conclusion from a raw numerical evaluation can be misleading. So, to verify if their performance differences are probably caused by randomness, four Pairwise T-Tests, a statistical test to determine if two paired sequences are significantly different, are conducted, testing the PSO FQ-ERG against the Lagrangian PSO, the DSA FQ-ERG against the Lagrangian DSA, the PSO FQ-ERG against the DSA FQ-ERG and the Lagrangian PSO against the DSA FQ-ERG. We have no reason to impose strict results, thus a significance level of 10% will be tolerated. On the Pairwise T-Tests, the null hypothesis is that the two paired samples are significantly different. The results of the Pairwise T-Tests are described in 4.3.

Sample 1	Sample 2	t-statistic	P-Value	Decision
PSO FQ-ERG	Lagrangian PSO	-0.56	0.58	Reject the Null Hypothesis
DSA FQ-ERG	Lagrangian DSA	13.76	0.00	Failed to Reject the Null Hypothesis
Lagrangian PSO	DSA FQ-ERG	-1.53	0.14	Reject the Null Hypothesis
PSO FQ-ERG	DSA FQ-ERG	-1.59	0.13	Reject the Null Hypothesis

Table 4.3 – Pairwise T-Test for the BD Rates of Proposed Algorithms (the baseline is the Baseline JPEG)

The Pairwise T-Test results show us that, while there is statistic significance to state that DSA FQ-ERG outperforms the Lagrangian DSA, from a statistical point, no claim comparing PSO FQ-ERG, Lagrangian PSO and DSA FQ-ERG can be made, despite a high tolerance level was set.

4.3 TIME PERFORMANCE

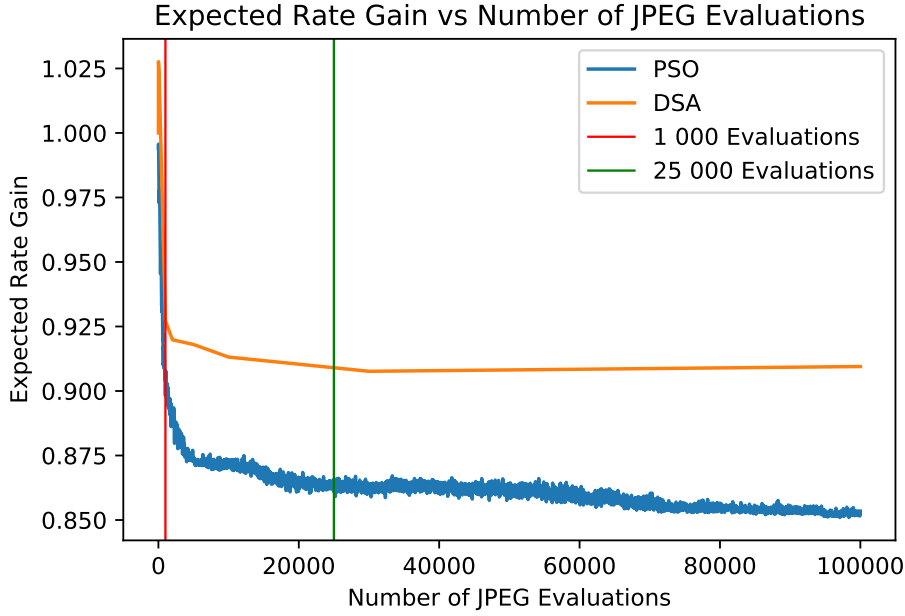


Figure 4.4 – Average ERG vs Number of JPEG Evaluations

The main drawback of adopting a nature-inspired metaheuristic to optimize quantization tables for image compression is that it is time-consuming. Even though using the vanilla quantization tables will probably raise a worse rate-distortion compromise than deploying one of the proposed optimization methods, it can be performed pretty fast, even in real-time, if proper JPEG accelerator hardware is present.

Therefore, although the proposed optimizations are still useful for offline applications regardless of the demanded time, its power is expanded if an improved rate-distortion compromise can be found in a relatively short amount of time, allowing the maximum number of JPEG evaluations allowed to be set according to the application and the available resources.

To shed a light on this issue, the relation between the average ERG and the number of JPEG evaluations on the optimization algorithm is represented in figure 4.4, revealing that, albeit the quantization optimization keeps increasing if more evaluations are performed, noticeable rate-distortion compromise gain can be obtained through few iterations, making the proposed methodology suitable even in near real-time or real-time applications, depending on the hardware capabilities available and the time constraints of the applications. It is also important to note that the expected time is expressed in the number of JPEG evaluations since the evaluation speed varies a lot according to the encoding implementations and the available hardware.

For testing and evaluation purposes, a limit of 1000 JPEG evaluations was set aiming to

obtain a good rate-distortion compromise in a moderate amount of time, emulating resource-scarce scenarios, such as computation in mobile phones or digital cameras. However, careful observation of the figure 4.4 suggests that, increasing the number of JPEG evaluations to up to 25000 may still be worthy if time is not critical to the application since there is an actual performance enhancement up to this point.

To provide a baseline estimative of clock time performance, both PSO and DSA were run over the entire Kodak Image Dataset, providing a fixed time budget for compressing each image (30, 90, and 300 seconds per image) for a quality factor of 75. The results are presented in table 4.4. The test was performed on an octa-core Intel i7-8550U CPU @ 1.8GHz and 16GB of RAM in our encoder, a highly-parallelized, albeit not optimized implementation that lies heavily in the DEAP and Scipy libraries in Python and the Independent JPEG Group's JPEG still image codec v9 encoder binary. No Graphics Processing Unit was employed to speed up the compression.

Method	Time	Compression Gain	PSNR Gain
PSO	30	4.6%	0.03dB
PSO	90	8.1%	0.08dB
PSO	300	11.3%	-0.01dB
DSA	30	3.2%	-0.08dB
DSA	90	7.3%	0.13dB
DSA	300	9.2%	0.06dB

Table 4.4 – Average Performance of a Fixed Time Compression on Kodak Dataset for Quality Factor = 75: Compression and PSNR Gains measured as the average gain across the dataset in comparison with the Baseline JPEG

4.4 VISUAL ASSESSMENT



Figure 4.5 – Image Kodak17 compressed with quantization table optimization (left) vs Image Kodak17 compressed with the vanilla quantization tables (right) for the same rate

Another interesting benchmark is a visual comparison between the compressed images generated using the optimized quantization tables and the vanilla quantization tables since while it is expected the chosen distortion metrics to be strongly correlated with human visual system perception, less distorted images do not necessarily mean images with higher perceptual quality.

For this reason, some image comparisons are provided in figures 4.5-4.6, contrasting the same rated images compressed with the optimized and vanilla quantization tables, allowing a direct assessment on whether the reductions on distortion caused by the optimized quantization tables were translated into visual enhancements.



Figure 4.6 – Image Kodak3 compressed with quantization table optimization (left) vs Image Kodak3 compressed with the vanilla quantization tables (right) for the same rate

One of the underlying assumptions of the quantization stage is that changes in some coefficients in the transformed domain are more noticeable than in others, which makes it logical to quantize less — it is, to attribute smaller values for the quantization coefficients — to coefficients that produce more noticeable differences, guaranteeing a finer-grained representation, while less noticeable coefficients are represented in fewer details.

Since the vanilla quantization tables attempt to propose a set of image independent, reasonable quantization coefficients, thus, not being able to benefit from image specific properties, investigating the distribution of the quantization table coefficients may provide us some insights of how the distortion is reduced. A careful analysis of the changes in the quantization tables is conducted investigating the aggregated luminance and chrominance tables for a quality factor of 50, exposed in figures 4.7 and 4.8.

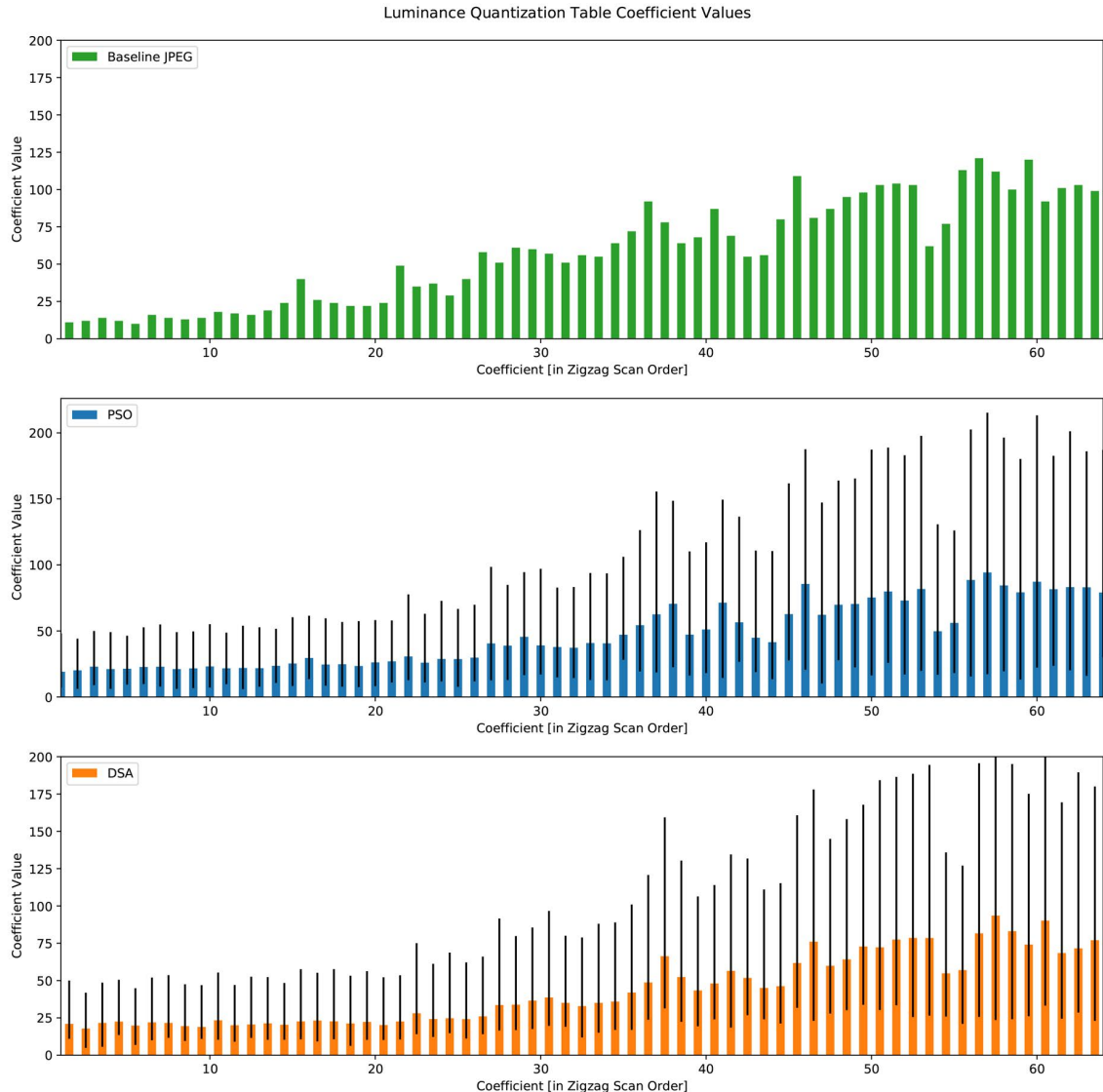


Figure 4.7 – Average Luminance Quantization Coefficients Values vs Transformed Coefficients in Zigzag Scan Order for the Kodak dataset with quality factor 50: Solid bars represent the average values, while error bars marks the excursion range, connecting the maximal and the minimal assumed values

The first thing that comes to our attention when scrutinizing the optimized quantization table for luminance is that the quantized coefficient values of the optimized tables are higher than the vanilla table ones for the first 16 coefficients, while there is a trend reversal for the other 48 coefficients, with the baseline JPEG assigning considerable higher values than the baseline JPEG. This works as evidence that the vanilla table may have been overestimating the actual importance of the first coefficients at the expense of the last coefficients, creating a scenario in which a more balanced distribution of the quantization coefficients, such as the optimized tables one, could raise better images, promoting a reduction in the distortion without increasing the image rate.

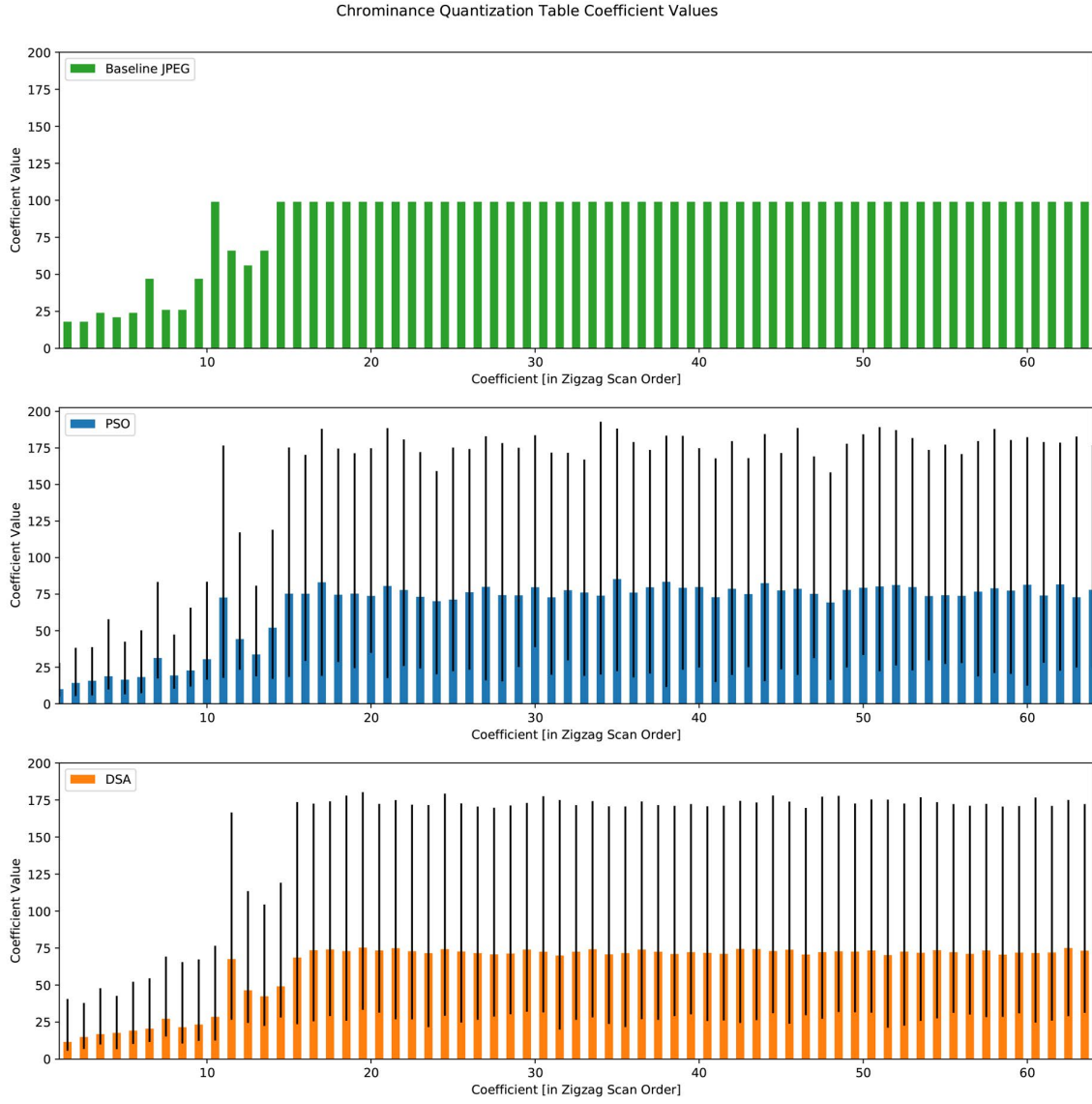


Figure 4.8 – Average Chrominance Quantization Coefficients Values vs Transformed Coefficients in Zigzag Scan Order for the Kodak dataset with quality factor 50: Solid bars represent the average values, while error bars marks the excursion range, connecting the maximal and the minimal assumed values

On the other hand, when inspecting the chrominance coefficient distribution, we can realize that the optimized quantization coefficients are smaller than the vanilla ones for every coefficient. Since luminance and chrominance table are jointly optimized, it may point out that the first coefficients overestimation is also at the expense of the chrominance coefficients.

Alternatively, these results may also signalize that the algorithm benefits from specific image proprieties. As the vanilla tables are designed to be generic and make no specific assumption on the image statistic characteristics, they fail to benefit of properties such as low variance, which, when known for a fact in beforehand, can allow a decrease in the quantization coefficients, as the entropy of the post-quantization coefficients will also be small.

Anyways, the error bars in both plots also show us that the flexibility to assign different values for each quantization coefficient according to image properties also plays an important part to justify the performance improvements, being very neat that, by allowing the coefficients to range from values lower to values higher than the ones in the vanilla table, it is possible to find better adjusts adaptively, deciding whether to lower or raise the quantization coefficient values based only in the rate-distortion trade-off.

5 CONCLUSION AND FUTURE WORK

For over 25 years, the JPEG has been the most widely adopted image compression standard in the world, leading to widespread hardware accelerator implementations in almost every image-related device. This universal availability of hardware accelerators gives the JPEG a considerable advantage in terms of performance against any new compression standard, since the hardware implementations ensure very fast JPEG encoding and decoding cycles.

In order to foster innovation, the JPEG standard did not specify a standard encoder, but rather just a standard decoder, so that every file that can be decoded by the JPEG decoder can be said to follow the JPEG file format. Since the JPEG standard defines support to custom quantization tables as one of its features, any optimization based just on custom quantization tables is still JPEG compliant and so can take advantage of the existing and widespread hardware support for JPEG.

This work discusses two nature-inspired meta-heuristics for JPEG image-specific quantization table optimization, as well as proposes a new metric that requires very few hyper-parameter tuning, describing a fast and automatic procedure for enhancing JPEG image compression.

It is shown that both Particle Swarm Optimization and Dual Simulated Annealing can obtain state-of-the-art performances when applied to optimize JPEG quantization tables, outperforming the baseline JPEG encoding, reducing the compressed file size at an average of 8% for same quality images.

Furthermore, both PSO and DSA behaviors are discussed in-depth, having their advantages and drawbacks pointed out and highlighted, allowing us to combine PSO's power in low rates with DSA outstanding performance in medium and high rates to obtain, choosing, pointwise, the best performing method, a hybrid method that outperforms baseline JPEG by 9.4% in terms of compression rate for same quality images.

Moreover, we also verify that our proposed new metric, FQ-ERG, despite requiring far less hyper-parameter tuning than the classic Lagrangian cost function, actually enhances considerably the performance of the DSA to optimize JPEG quantization tables, while, in PSO, the difference of performance when optimizing FQ-ERG and the Lagrangian cost function was negligible under a 10% significance level, suggesting that the proposed new metric is a suitable option for a JPEG encoder that incorporates by default the quantization table optimization.

An evaluation of the proposed method in terms of resource consumption is also provided,

with a detailed speed-performance trade-off curve being drawn, helping to guide the design of applications for obtaining the best performance meets the specific time and hardware constraints. The number of 1000 evaluations was determined to be reasonable when time is a bottleneck, while consistent performance increase was noticed up to 25000 evaluations, which was determined as our threshold for high-performing, offline applications.

These results also pave the way for further research exploring potential improvements on JPEG compression driven by nature-inspired algorithms, such as, for example, performing a joint optimization of the applied transform, quantization, and entropy encoding tables, or by employing different black-box optimization techniques to perform this joint optimization.

Promising studies can also be conducted in developing fast or real-time solutions to quantization table optimization, since a lot of digital image applications require real-time or near real-time compression. Last, but not least, the design of new rate-distortion metrics for nature-inspired quantization table optimization also seems an interesting alternative to obtain performance enhancements, since our results suggest that an appropriate choice for the fitness function may play a leading role optimization.

BIBLIOGRAPHY

- 1 BENAVIDES, E. *Players of Brazil's Flamengo celebrate on the podium with the trophy after winning the Copa Libertadores.* AFP. Disponível em: <https://ogimg.infoglobo.com.br/in/24097539-f64-d49/FT1086A/652/85843852_Players-of-Brazils-Flamengo-celebrate-on-the-podium-with-the-trophy-after-winning-the-Copa.jpg>.
- 2 HUDSON, G. et al. JPEG at 25: Still going strong. *IEEE MultiMedia*, Institute of Electrical and Electronics Engineers (IEEE), v. 24, n. 2, p. 96–103, abr. 2017.
- 3 HUDSON, G. et al. JPEG-1 standard 25 years: past, present, and future reasons for a success. *Journal of Electronic Imaging*, SPIE-Intl Soc Optical Eng, v. 27, n. 04, p. 1, ago. 2018.
- 4 ELBADRI, M. et al. Hardware support of JPEG. In: *Canadian Conference on Electrical and Computer Engineering, 2005*. [S.l.]: IEEE.
- 5 WALLACE, G. K. The JPEG still picture compression standard. *Communications of the ACM*, Association for Computing Machinery (ACM), v. 34, n. 4, p. 30–44, abr. 1991.
- 6 R., A. et al. A machine learning approach for removal of jpeg compression artifacts: A survey. *International Journal of Computer Applications*, v. 138, p. 24–28, 03 2016.
- 7 AL-NUAIMI, A. H. H.; AL-JUBOORI, S. S.; MOHAMMED, R. J. Image compression using proposed enhanced run length encoding algorithm. 2018.
- 8 Yang, E.; Wang, L. Joint optimization of run-length coding, huffman coding, and quantization table with complete baseline jpeg decoder compatibility. *IEEE Transactions on Image Processing*, v. 18, n. 1, p. 63–74, 2009.
- 9 Zhang, X. et al. Just-noticeable difference-based perceptual optimization for jpeg compression. *IEEE Signal Processing Letters*, v. 24, n. 1, p. 96–100, 2017.
- 10 Ratnakar, V.; Livny, M. Extending rd-opt with global thresholding for jpeg optimization. In: *Proceedings of Data Compression Conference - DCC '96*. [S.l.: s.n.], 1996. p. 379–386.
- 11 CHAO, J.; CHEN, H.; STEINBACH, E. On the design of a novel JPEG quantization table for improved feature detection performance. In: *2013 IEEE International Conference on Image Processing*. [S.l.]: IEEE, 2013.
- 12 EDMUNDSON, D.; SCHAEFER, G. Exploiting JPEG compression for image retrieval. In: *2012 IEEE International Symposium on Multimedia*. [S.l.]: IEEE, 2012.
- 13 JIANG, Y.; PATTICHIS, M. S. JPEG image compression using quantization table optimization based on perceptual image quality assessment. In: *2011 Conference Record of the Forty Fifth Asilomar Conference on Signals, Systems and Computers (ASILOMAR)*. [S.l.]: IEEE, 2011.

- 14 AND, S. N. A literature review on quantization table design for the JPEG baseline algorithm. *International Journal Of Engineering And Computer Science*, Valley International, ago. 2016.
- 15 GRADIENT Descent for Non-convex Problems in Modern Machine Learning. Figshare, 2019.
- 16 STRONGIN, R. G. *Global optimization with non-convex constraints : sequential and parallel algorithms*. Dordrecht Boston: Kluwer Academic Publishers, 2000. ISBN 978-1-4615-4677-1.
- 17 MORÉ, J. J.; WILD, S. M. Benchmarking derivative-free optimization algorithms. *SIAM Journal on Optimization*, Society for Industrial & Applied Mathematics (SIAM), v. 20, n. 1, p. 172–191, jan. 2009.
- 18 VISWAJAA, S.; BALASUBRAMANIAN, V.; KARPAGAM, G. A survey on nature inspired meta-heuristics algorithms in optimizing the quantization table for the jpeg baseline algorithm. *International Advanced Research Journal in Science, Engineering and Technology*, v. 2, p. 114–123, 01 2015.
- 19 KENNEDY, J.; EBERHART, R. Particle swarm optimization. In: *Proceedings of ICNN'95 - International Conference on Neural Networks*. IEEE. Disponível em: <<https://doi.org/10.1109/icnn.1995.488968>>.
- 20 XIANG, Y. et al. Generalized simulated annealing algorithm and its application to the thomson model. *Physics Letters A*, Elsevier BV, v. 233, n. 3, p. 216–220, ago. 1997.
- 21 ONNASCH, D.; PRAUSE, G.; PLOGER, A. Quantization table design for JPEG compression of angiographic images. In: *Computers in Cardiology 1994*. IEEE Comput. Soc. Press. Disponível em: <<https://doi.org/10.1109/cic.1994.470199>>.
- 22 Costa, L. F.; Veiga, A. C. P. Identification of the best quantization table using genetic algorithms. In: *PACRIM. 2005 IEEE Pacific Rim Conference on Communications, Computers and signal Processing, 2005*. [S.l.: s.n.], 2005. p. 570–573.
- 23 Tuba, M.; Bacanin, N. Jpeg quantization tables selection by the firefly algorithm. In: *2014 International Conference on Multimedia Computing and Systems (ICMCS)*. [S.l.: s.n.], 2014. p. 153–158.
- 24 TUBA, E. et al. JPEG quantization table optimization by guided fireworks algorithm. In: *Lecture Notes in Computer Science*. [S.l.]: Springer International Publishing, 2017. p. 294–307.
- 25 KUMAR, B. V.; KARPAGAM, M. Differential evolution versus genetic algorithm in optimising the quantisation table for JPEG baseline algorithm. *International Journal of Advanced Intelligence Paradigms*, Inderscience Publishers, v. 7, n. 2, p. 111, 2015. Disponível em: <<https://doi.org/10.1504/ijaip.2015.070766>>.
- 26 Kumar, B. V.; Karpagam, G. R.; Naresh, S. P. Generation of jpeg quantization table using real coded quantum genetic algorithm. In: *2016 International Conference on Communication and Signal Processing (ICCSP)*. [S.l.: s.n.], 2016. p. 1705–1709.

- 27 LI, X.; WANG, J. A steganographic method based upon jpeg and particle swarm optimization algorithm. *Inf. Sci.*, v. 177, p. 3099–3109, 08 2007.
- 28 FAZLI, S.; KIAMINI, M. A high_performance steganographic method using JPEG and PSO algorithm. In: *2008 IEEE International Multitopic Conference*. [S.l.]: IEEE, 2008.
- 29 SNASEL, V. et al. JPEG steganography with particle swarm optimization accelerated by AVX. *Concurrency and Computation: Practice and Experience*, Wiley, v. 32, n. 8, jul. 2019.
- 30 RABEVOHITRA, F. H.; SANG, J. High capacity steganographic scheme for JPEG compression using particle swarm optimization. *Advanced Materials Research*, Trans Tech Publications, Ltd., v. 433-440, p. 5118–5122, jan. 2012.
- 31 ABBOOD, A. S. Design of jpeg image compression scheme with a particle swarm optimization-based quantization table. *International journal of innovation and scientific research*, v. 25, p. 22–31, 2016.
- 32 HOPKINS, M.; MITZENMACHER, M.; WAGNER-CARENA, S. *Simulated Annealing for JPEG Quantization*. 2017.
- 33 GONZALEZ, R. *Digital image processing*. New York, NY: Pearson, 2018. ISBN 978-0133356724.
- 34 KNUDSEN, J. *Java 2D graphics*. Beijing Sebastopol, Calif: O'Reilly, 1999. ISBN 1-56592-484-3.
- 35 LZ, H. *Industrial color testing : fundamentals and techniques*. Weinheim New York: Wiley-VCH, 2001. ISBN 3-527-30436-3.
- 36 HIRSCH, R. *Exploring colour photography : a complete guide*. London: Laurence King, 2005. ISBN 1-85669-420-8.
- 37 JACK, K. *Video demystified : a handbook for the digital engineer*. Amsterdam Boston: Newnes/Elsevier, 2007. ISBN 978-0-7506-8395-1.
- 38 Chan, G. Toward better chroma subsampling: Recipient of the 2007 smpte student paper award. *SMPTE Motion Imaging Journal*, v. 117, n. 4, p. 39–45, 2008.
- 39 ITU, T. S. S. O. *ITU-T Recommendation T.871 : SERIES T: TERMINALS FOR TELEMATIC SERVICES Still-image compression – JPEG-1 extensions*. [S.l.], 2011.
- 40 KHOKHAR, M. J.; EHLINGER, T.; BARAKAT, C. From network traffic measurements to QoE for internet video. In: *2019 IFIP Networking Conference (IFIP Networking)*. IEEE, 2019. Disponível em: <<https://doi.org/10.23919/ifipnetworking.2019.8816854>>.
- 41 SAYOOD, K. *Introduction to Data Compression*. [S.l.]: Elsevier - Morgan Kaufmann, 2012.
- 42 ITU-T.81. Information technology –digital compression and coding of continuous-tone still images: – requirements and guidelines.

- 43 SKODRAS, A.; CHRISTOPOULOS, C.; EBRAHIMI, T. The JPEG 2000 still image compression standard. *IEEE Signal Processing Magazine*, Institute of Electrical and Electronics Engineers (IEEE), v. 18, n. 5, p. 36–58, 2001. Disponível em: <<https://doi.org/10.1109/79.952804>>.
- 44 WALLACE, G. The JPEG still picture compression standard. *IEEE Transactions on Consumer Electronics*, Institute of Electrical and Electronics Engineers (IEEE), v. 38, n. 1, p. xviii–xxxiv, 1992. Disponível em: <<https://doi.org/10.1109/30.125072>>.
- 45 RASHID, A.; CHRISTINE, G.; NASIR, M. Lossy image compression: JPEG and JPEG2000 standards. In: *Handbook of Image and Video Processing*. Elsevier, 2005. p. 709–XXII. Disponível em: <<https://doi.org/10.1016/b978-012119792-6/50105-4>>.
- 46 LEHMANN, E. L. *Theory of point estimation*. New York: Springer, 1998. ISBN 978-0-387-98502-2.
- 47 BERMEJO, S.; CABESTANY, J. Oriented principal component analysis for large margin classifiers. *Neural Networks*, Elsevier BV, v. 14, n. 10, p. 1447–1461, dez. 2001.
- 48 GUPTA, P. et al. A novel full-reference image quality index for color images. In: _____. [S.l.: s.n.], 2012. v. 132, p. 245–253.
- 49 Wang, Z.; Bovik, A. C. Mean squared error: Love it or leave it? a new look at signal fidelity measures. *IEEE Signal Processing Magazine*, v. 26, n. 1, p. 98–117, 2009.
- 50 SALOMON, D. *Data compression : the complete reference*. London: Springer, 2007. ISBN 978-1846286025.
- 51 Huynh-Thu, Q.; Ghanbari, M. Scope of validity of psnr in image/video quality assessment. *Electronics Letters*, v. 44, n. 13, p. 800–801, 2008.
- 52 Li, X. et al. Lagrange multiplier selection for rate-distortion optimization in svc. In: *2009 Picture Coding Symposium*. [S.l.: s.n.], 2009. p. 1–4.
- 53 HOANG, D. T.; LONG, P. M.; VITTER, J. S. titlerate-distortion optimizations for motion estimation in low-bit-rate video coding/title. In: BHASKARAN, V.; SIJSTERMANS, F.; PANCHANATHAN, S. (Ed.). *Digital Video Compression: Algorithms and Technologies 1996*. [S.l.]: SPIE, 1996.
- 54 G., B. Improvements of the bd-psnr model. 2008.
- 55 EBERHART, R.; KENNEDY, J. A new optimizer using particle swarm theory. In: *MHS95. Proceedings of the Sixth International Symposium on Micro Machine and Human Science*. [S.l.]: IEEE.
- 56 ALMEIDA, B. S. G. de; LEITE, V. C. Particle swarm optimization: A powerful technique for solving engineering problems. In: *Swarm Intelligence - Recent Advances, New Perspectives and Applications*. [S.l.]: IntechOpen, 2019.
- 57 ZHANG, Y.; WANG, S.; JI, G. A comprehensive survey on particle swarm optimization algorithm and its applications. *Mathematical Problems in Engineering*, v. 2015, p. 1–38, 2015.

- 58 POLI, R.; KENNEDY, J.; BLACKWELL, T. Particle swarm optimization. *Swarm Intelligence*, Springer Science and Business Media LLC, v. 1, n. 1, p. 33–57, ago. 2007.
- 59 TRELEA, I. C. The particle swarm optimization algorithm: convergence analysis and parameter selection. *Information Processing Letters*, Elsevier BV, v. 85, n. 6, p. 317–325, mar. 2003. Disponível em: <[https://doi.org/10.1016/s0020-0190\(02\)00447-7](https://doi.org/10.1016/s0020-0190(02)00447-7)>.
- 60 EBERHART, R.; SHI, Y. Comparing inertia weights and constriction factors in particle swarm optimization. In: *Proceedings of the 2000 Congress on Evolutionary Computation. CEC00 (Cat. No.00TH8512)*. [S.I.]: IEEE.
- 61 CAZZANIGA, P.; NOBILE, M. S.; BESOZZI, D. The impact of particles initialization in PSO: Parameter estimation as a case in point. In: *2015 IEEE Conference on Computational Intelligence in Bioinformatics and Computational Biology (CIBCB)*. [S.I.]: IEEE, 2015.
- 62 CLERC, M.; KENNEDY, J. The particle swarm - explosion, stability, and convergence in a multidimensional complex space. *IEEE Transactions on Evolutionary Computation*, Institute of Electrical and Electronics Engineers (IEEE), v. 6, n. 1, p. 58–73, 2002.
- 63 TAHERKHANI, M.; SAFABAKHSH, R. A novel stability-based adaptive inertia weight for particle swarm optimization. *Applied Soft Computing*, Elsevier BV, v. 38, p. 281–295, jan. 2016.
- 64 SARKAR, S.; ROY, A.; PURKAYASTHA, B. S. Application of particle swarm optimization in data clustering: A survey. *International Journal of Computer Applications*, v. 65, p. 38–46, 2013.
- 65 TSALLIS, C. Possible generalization of boltzmann-gibbs statistics. *Journal of Statistical Physics*, Springer Science and Business Media LLC, v. 52, n. 1-2, p. 479–487, jul. 1988.
- 66 TSALLIS, C.; STARIOLO, D. A. Generalized simulated annealing. *Physica A: Statistical Mechanics and its Applications*, Elsevier BV, v. 233, n. 1-2, p. 395–406, nov. 1996.
- 67 XIANG, Y.; GONG, X. G. Efficiency of generalized simulated annealing. *Physical Review E*, American Physical Society (APS), v. 62, n. 3, p. 4473–4476, set. 2000.
- 68 MULLEN, K. M. Continuous global optimization inR. *Journal of Statistical Software*, Foundation for Open Access Statistic, v. 60, n. 6, 2014.
- 69 Y. GUBIAN S., S. B. X.; J., H. Generalized simulated annealing for efficient global optimization: the gensa package for r. *The R Journal*, Foundation for Open Access Statistic, v. 5, n. 1, 2013.
- 70 GROUP, I. The independent jpeg group's jpeg software. 03 2004.
- 71 FORTIN, F.-A. et al. DEAP: Evolutionary algorithms made easy. *Journal of Machine Learning Research*, v. 13, p. 2171–2175, jul 2012.
- 72 VIRTANEN, P. et al. SciPy 1.0: fundamental algorithms for scientific computing in python. *Nature Methods*, Springer Science and Business Media LLC, v. 17, n. 3, p. 261–272, fev. 2020.

APPENDIX

A RATE-DISTORTION CURVES ON KODAK DATASET

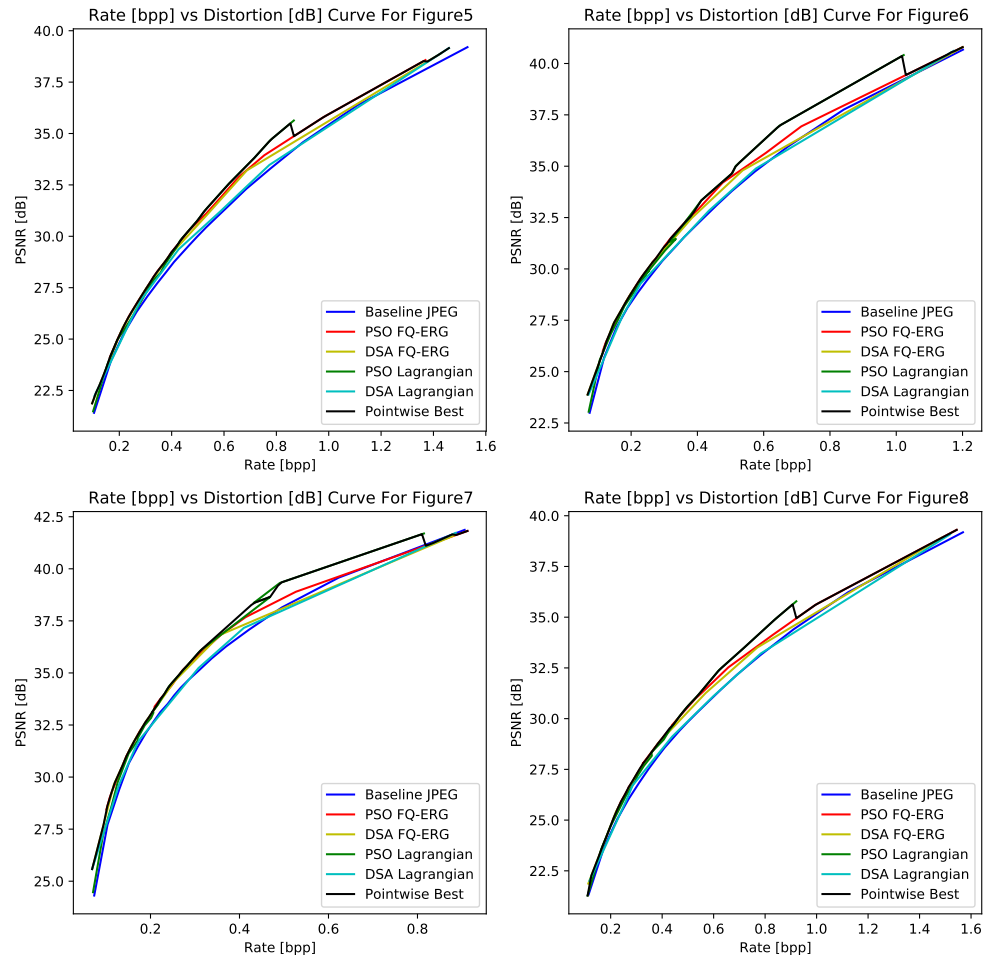


Figure A.1 – Rate-Distortion Curve for the Images Kodak5-Kodak8

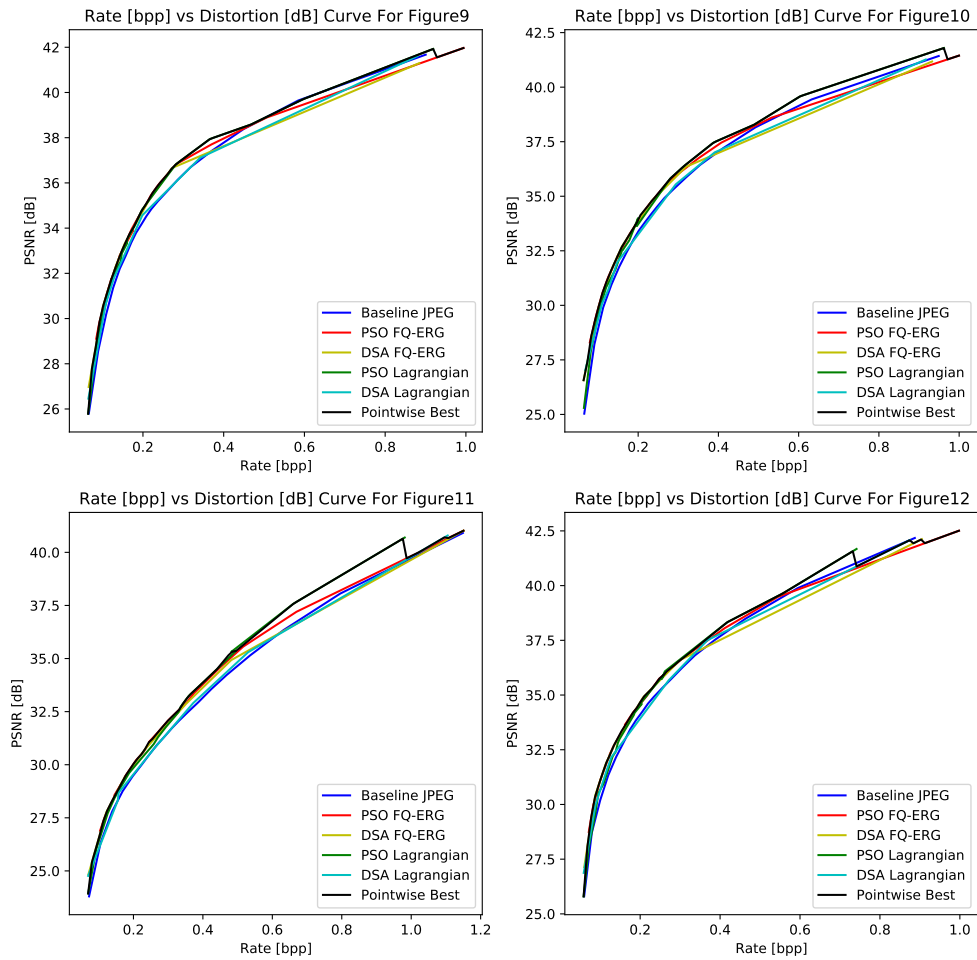


Figure A.2 – Rate-Distortion Curve for the Images Kodak9-Kodak12

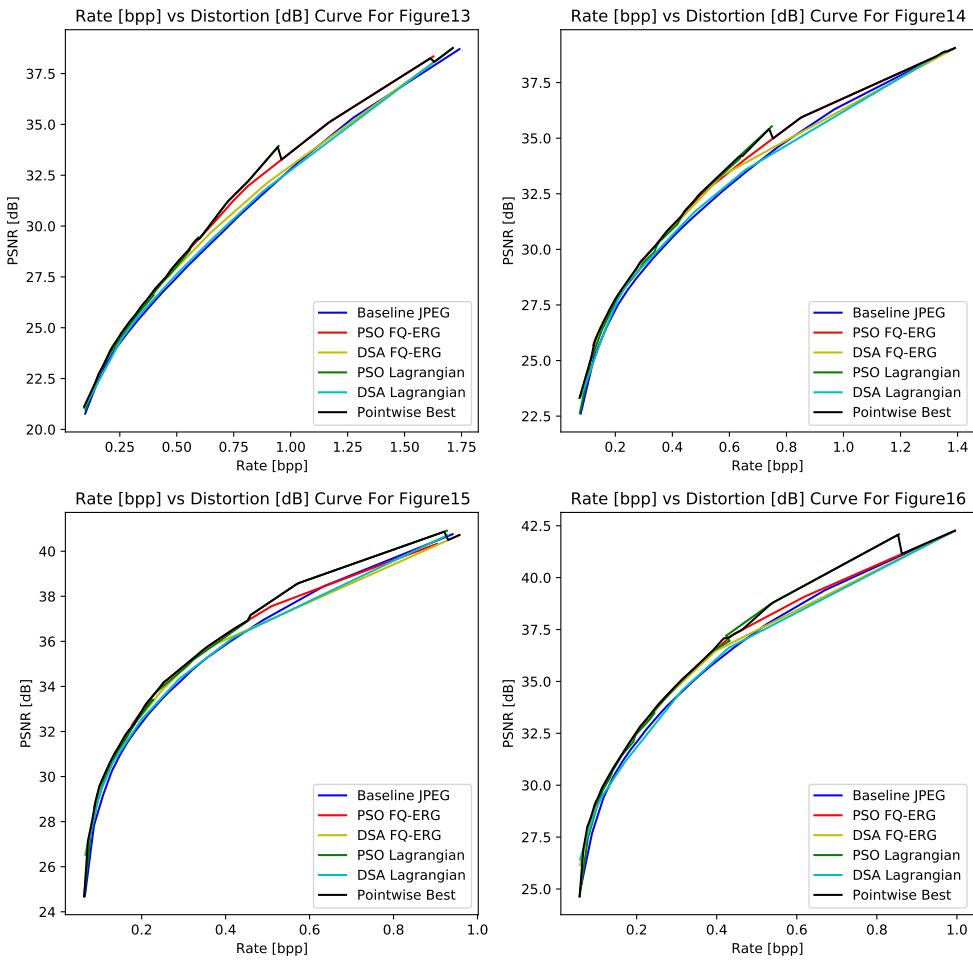


Figure A.3 – Rate-Distortion Curve for the Images Kodak13-Kodak16

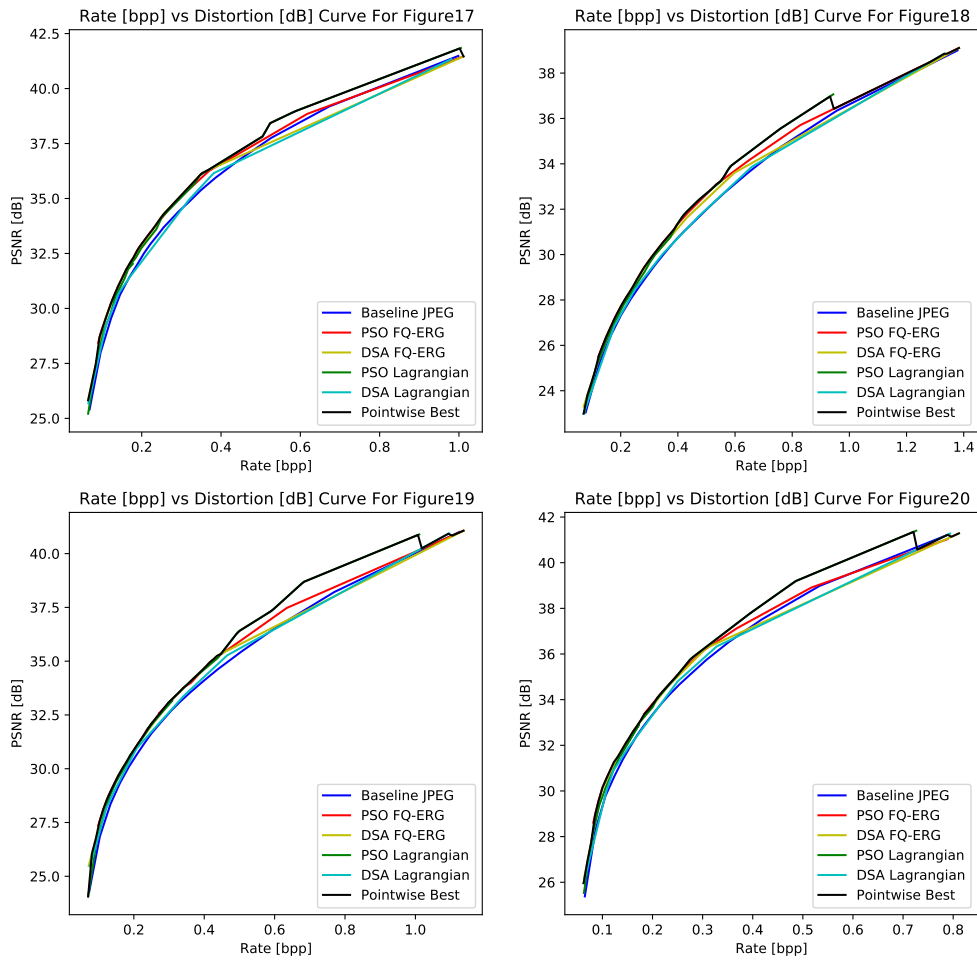


Figure A.4 – Rate-Distortion Curve for the Images Kodak17-Kodak20

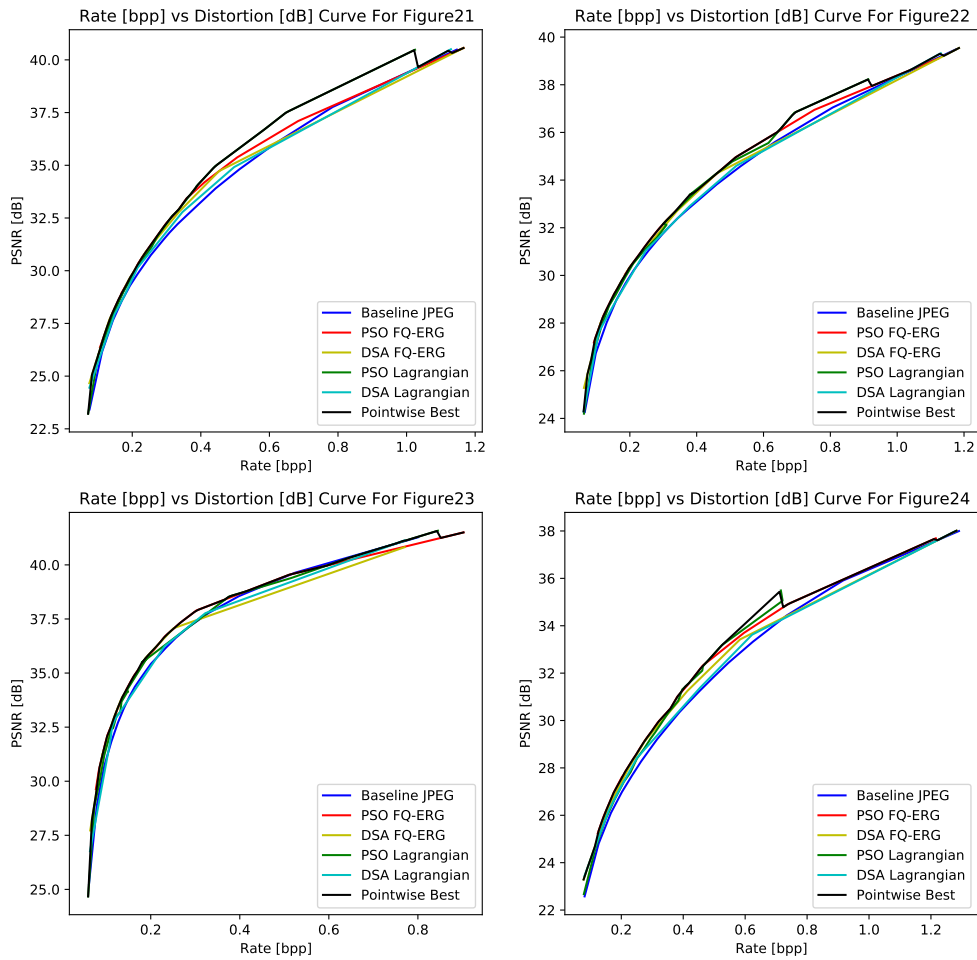


Figure A.5 – Rate-Distortion Curve for the Images Kodak21-Kodak24